We thank the referee for the thorough review and constructive comments. Please find below detailed responses to each comment or question, including notations of improvements to the manuscript. Referee comments are in blue fonts. Changes to the text are highlighted in yellow.

Referees' comments:

Referee #1:

Review of

Cloud droplet activation of secondary organic aerosol is mainly controlled by molecular weight, not water solubility

Wang, Shilling, Liu et al. showcase a series of experiments measuring organic aerosol hygroscopicity expressed as κCCN, org using a condensation particle counter and a CCN counter. Their chamber experiments span common SOA precursors with varying inorganic (ammonium sulphate) to organic volume ratios. To explain the experimental results, the authors use previously published relationships for volatility to molecular weight and κCCN, org to molecular weight. They presented an analysis of the major factors affecting the hygroscopicity parameter of the organic aerosol formed, assuming complete dissolution at high relative humidity (RH). The molecular weight of the organic compounds is highlighted as a major factor in determining the apparent hygroscopicity parameter at high RH.

This work is well within the scope of Atmospheric Chemistry and Physics, and is of general interest to the community and discusses new findings. The paper is based on solid experimental work which is largely described in the Supplementary Information, some of which is suggested to be moved into the main manuscript. However, in this referee's opinion, the presentation of the findings and the logic of the explanations reveal a lack of clarity and certain flaws in the argumentation that should (and can) be addressed. Therefore, the manuscript requires major revisions and additional supporting evidence for the assumptions made. More clarity is especially needed for the definition and use of the terms 'water solubility' and 'hygroscopicity' as pointed out below. The organic hygroscopicity addressed in this paper specifically targets the high relative humidity or supersaturated regime. There needs to be an increased specificity on where, at approximately infinite dilution, the presented modeling results and the provided interpretation apply. The paper also needs more specificity in the use and validity of Eq. (2). General and specific comments are detailed in the following.

General comments

1. Clarity on Hygroscopicity Needed:

Hygroscopicity is a nebulous term which needs to be defined. Hygroscopicity can be defined as the mass of water per mass of solute at a given RH or water activity or the equivalent ratios using moles or volumes – or in a different way. Hygroscopicity is not equal to κCCN, org, but the authors implicitly assume just that (page 3 line 19) and elsewhere in the manuscript. Introducing and defining κ as a hygroscopicity parameter should be added to the introduction. Moreover, κ is not a material constant, since in reality, it may depend on the relative humidity range. For example, changes in κ as a function of RH for different SOA have been shown, among others, by Rastak et al. (2017).

The authors need to specify that their measurements are κ at CCN activation (i.e., κCCN, org) and do not directly translate to subsaturated hygroscopic growth factors (κHGF, org). Therefore, the papers title and main conclusion do not apply to subsaturated RH conditions. From the context of the measurements, I can infer that the discussion is on κCCN, org, but the reader should not have to do that.

The hygroscopicity parameter κ is now introduced in the introduction section. We also clarified that κ derived from the measurements represent values at droplet activation and may be different from those associated with hygroscopic growth under sub-saturated conditions.

2. Clarity on Solubility Needed:

Water-solubility is not currently defined in the introduction. It can either be the solute saturation point (limit of solubility) of a solid-liquid equilibrium or it could refer to the transition from liquid-liquid equilibrium (miscibility limitation as mentioned in the supplementary information) to a single aqueous phase. The solubility values of those variants likely differ and, according to equilibrium thermodynamics, depend on the other species in an aqueous solution. Providing a quantitative definition earlier in the paper (currently one needs to read until page 9 to find one), would also help distinguishing the differences between water-solubility (C), and apparent κCCN, org. The introduction would benefit from having the general definition of hygroscopicity early on. This change will make it clear to the reader that organic hygroscopicity may change over the full water activity range, complete dissolution occurs at some RH value, depending on the other mixture species, and κCCN, org is at water supersaturation RH.

Water-solubility is now defined in the introduction.

"Water solubility is defined as the amount solute that can dissolve in water at saturation, corresponding to solid/aqueous solution equilibrium. Miscibility is related to solubility and refers to the ability of two liquid phases to mix. Miscibility limitation leads to liquid-liquid phase separation (LLPS). If LLPS occurs under supersaturated conditions, miscibility can exert similar control on droplet activation as water solubility…"

We also clarified that hygroscopicity parameter κ may vary with relative humidity. The κ values examined in this study are at droplet activation under supersaturated conditions, and they may be different from those under sub-saturated conditions associated with particle hygroscopic growth.

On a related point, in the SI (section 6, page 12, line 20) the authors assumed miscibility transition of 0.5 O:C, does this include a salting-out effect or does it assume only water-organics phase separation? In this discussion on miscibility, the observational work performed by Renbaum-Wolff et al. (2016) on SOA liquid–liquid phase separation at high relative humidities should be included.

We referenced Renbaum-Wolff et al. (2016) in the discussion of miscibility and LLPS. The assumed transition of 0.5 O:C does not include the salting out effect. Since functional group composition is a more relevant measure than O:C, we also rephrased the sentence as follows:

Model calculations and experimental data suggest that adding a few hydroxyl and/or carboxylic acid groups is enough to remove miscibility limitations (Bertram et al., 2011; Petters et al., 2016) for pure organic compounds at water activity corresponding to supersaturated conditions, consistent with the results from our experiments.

Could the authors add some discussion on how the interpretation would change (or not) if the particles were phase-separated (water and organic-rich phases) during the CCN measurement? Especially, given the context of recently published work by Ovadnevaite et al. (2017) on phase-separated CCN activation.

This relevant discussion of the LLPS is already included in the supplementary information:

Miscibility is related to solubility and refers to the ability of two liquid phases to mix. Substances that form two liquid phases are immiscible. If a miscibility transition occurs in the supersaturated regime, miscibility limitations exert a similar control over critical supersaturation as solubility (Petters et al., 2006; Petters et al., 2016), i.e., the effective hygroscopicity κ_{org} observed from

CCN activation is reduced at lower net water contents (smaller size or less hygroscopic material present). Distinguishing between miscibility and solubility in CCN experiments is not possible because the manifestation of the effect is identical.

The above discussion is now moved to main text following the suggestion of referee.

…

Ovadnevaite et al. (2017) suggested that LLPS leads to complete or partial engulfing of a hygroscopic particle core by a hydrophobic organic-rich phase. This results in substantial decrease of surface tension without a reduction of the Raoult's effect, leading to higher CCN activity. Simulations based on this LLPS model suggest the effect of reduced surface tension on CCN activity is more pronounced for ultrafine particles, and the effect is much weaker for particles with larger diameters studied here. One prediction of the model is that particles with different organics to sulfate mass ratios (i.e. sulfate volume fraction) exhibit similar effective hygroscopicity parameter. Such behavior is explained by that a decrease in sulfate content, and therefore the Raoult's effect, is compensated for by a prolonged surface tension lowering (to larger diameters during droplet activation) due to a larger relative amount of organics (Ovadnevaite et al., 2017). This trend is very different from the results of SOA examined in this study, which show a nearly constant κ_{org} therefore lower effective hygroscopicity parameter for particles with high organics to sulfate mass ratio.

3. Community claims need support and clarification:

The statement on page 4 line 9-12 needs a justification, as well as a similar statement in the abstract (page 2 line 13-15): "Earlier studies showed organic hygroscopicity increases nearly linearly with oxidation level. Such increase of hygroscopicity is conventionally attributed to higher water solubility for more oxidized organics.". Claiming that an increase in polarity leads to an increased solubility and then higher κCCN, org is a "long held hypothesis" needs to be corroborated by citation of relevant references. At least this referee does not share the opinion that the higher water-solubility was the main hypothesis in "the community". Jimenez et al. (2015) showed a relation between O:C and κCCN, org , whereas Riipinen et al. (2015) showed a relation between solubility and κCCN, org. There is no citation provided linking O:C and solubility. On page 4 line 14-16, the citation Kuwata et al. (2013) does show a loose trend of O:C with κCCN, org, but the author's statement neglects the fact that molar mass as well as density are changing with O:C. In the same sentence, the Petters et al. (2009) citation is confusing; as

Petters et al. (2009) does not discuss the oxidation level, but discusses molar volume. If the authors are reinterpreting the results of Petters et al., (2009) and Petters et al., (2016) through an O:C lens and neglecting the covarying molar mass that should be stated.

An increase in organic polarity could increase water affinity, but to change solubility, the molecular size and, for solid-liquid solubility, the crystal structure, is also playing an important role (e.g. consider the well-known odd-even alteration with carbon atom number in the water-solubilities of dicarboxylic acids; e.g. Bilde et al., 2003). Changes to solubility would depend on the combination of molecular size, molecular interactions in solution, which would include polarity, and crystal structure (unless liquid-liquid miscibility is meant).

We thank the referee for this comment. The text is revised to:

Several studies show that for ambient organic aerosols and laboratory generated secondary organic aerosols (SOA), organic hygroscopicity parameter increases nearly linearly with the atomic O:C ratio (e.g., Jimenez et al., 2009;Lambe et al., 2011), a parameter commonly used to quantify oxidation level of organics. For single component aerosols and simple mixtures, the effect of increasing oxidation level on water solubility and in turn hygroscopicity is well established (Petters et al., 2009;Petters et al., 2016;Rickards et al., 2013;Kuwata et al., 2013). Water solubility is defined as the amount solute that can dissolve in water at saturation, corresponding to solid/aqueous solution equilibrium. Miscibility is related to solubility and refers to the ability of two liquid phases to mix. Miscibility limitation leads to liquid-liquid phase separation (LLPS). If LLPS occurs under supersaturated conditions, miscibility can exert similar control on droplet activation as water solubility (Petters et al., 2006;Petters et al., 2016), and is further discussed in a later section. Kuwata et al. (2013) shows that for single organic compounds, water solubility generally increases with O:C. One plausible explanation is that as organic molecules become increasingly oxidized (i.e., increased O:C ratio), they are more polar, leading to increased water solubility. As O:C increases from near zero, the regime for the activation of single organic compound transitions from insoluble, to slightly soluble, then to highly soluble, leading to a general increasing trend of hygroscopicity parameter (Kuwata et al., 2013). In the highly soluble regime, the hygroscopicity parameter is no longer limited by water solubility, but controlled mainly by molecular weight instead (e.g., Kuwata et al., 2013). Nakao (2017) modeled the hygroscopicity of secondary organic species, and the results suggest the increase of organic hygroscopicity with O:C is likely due to a combination of both increased water solubility and variation in volatility that determines the molecular size of dissolved solute. Riipinen et al. (2015) examined cloud activation of multicomponent organic particles theoretically and suggested that the organic hygroscopicity parameter is strongly influenced by the distributions of species with water solubility between 0.1 and 100 g L^{-1}, i.e., the range for slightly soluble species. Whereas all the above studies suggest that the hygroscopicity parameter is strongly influenced by water solubility of slightly soluble organics, for ambient organic aerosols and laboratory generated secondary organic aerosols, the influence of water solubility on organic hygroscopicity has not been systematically examined experimentally, and the underlying mechanism for the increasing hygroscopicity with increasing O:C remains unclear.

4. More Support for Eq. 2:

The applicability and usability range of Eq. 2 needs to be discussed. This discussion is even more warranted since Sullivan et al. (2009) used Eq. 2 for mineral dust, not organic molecules.

Starting with the definition of κ from Petters and Kreidenweis (2007) (their Eq. 2), one can derive Eq. 2 shown in this manuscript as a limiting case. Note, one must substitute water activity for the water mole fraction and activity coefficient. In doing this, one can show the assumption of i = 1 is valid only under conditions of high dilution in water, when the activity coefficient and the mole fraction of water each approach one. Due to the activity coefficient being depended on the organic's O:C and molecular structure, it is likewise true that i is also dependent on those same properties in non-dilute cases. Such a derivation and pertinent discussion would make the origin and limited range of application of Eq. (2) clear. This is important since much of the argumentation about the role of molecular weight (i.e. molar mass) is built based on assuming Eq. (2) to be valid or at least to be a valid approximation.

We agree and clarified that Eq. 2 describes intrinsic hygroscopicity parameter at droplet activation. We also included the following discussion in the text:

The assumption of *i*=1 is valid only under conditions of high dilution in water, such as at droplet activation under supersaturated conditions.

The authors should add more to the discussion of the previous uses of Eq. 2. In the paper's current state, the reader could have the impression that the control of κCCN, org by Morg is a brand new discovery. That impression would be incorrect when we consider the following quotation:

"For highly soluble particles, CCN activity is dominantly controlled by molar volume, which is determined by both ρorg and 1/Morg (Eq. 5) (Petters et al., 2009a). Kuwata et al. (2012) developed a method to predict ρorg using O : C and H : C ratios. According to the method, ρorg is higher for highly oxygenated compounds. Even so, the range in ρorg values for O : C>0.6 from 1100 to 1650 kgm−3 is not sufficient to explain the variability observed for κ for highly soluble materials. Furthermore, the ρorg values of carbohydrates and synthetic polymers do not vary significantly yet the variations in κ is significant (cf. Supplement). The implication is that the dominant regulator of CCN activity is Morg for highly soluble particles."

-Kuwata et al., 2013

The authors' experimental work does extend the above result by Kuwata et al. (2013) to SOA systems. But, the authors did not place their results within the context of the previously published work, which similarly uses Eq. 2 with organic compounds.

The following text is in the original text:

In the absence of solubility limitation, κ_{org} is essentially the same as $\kappa_{org,intr,}$ and is controlled mainly by molar volume (Eq. 2). This has been shown by earlier studies for pure organic compounds with sufficient solubility (Kuwata et al., 2013; Petters et al., 2009; Petters et al., 2016).

We also added the following sentences in the introduction:

As O:C increases from near zero, the regime for the activation of single organic compound transitions from insoluble, to slightly soluble, then to highly soluble, leading to a general increasing trend of hygroscopicity parameter (Kuwata et al., 2013). In the highly soluble regime, the hygroscopicity parameter is no longer limited by water solubility, but controlled mainly by molecular weight instead (Kuwata et al., 2013).

Also, it is clear that assuming density of organics to remain constant upon oxidation is only an approximation, since with increases in O:C and molar mass, density may also vary by up to ~ 40 %.

Following discussion is now included:

As shown by Kuwata et al. (2013), the variation of organic density with O:C is relatively weak and can't explain the variation in κ_{org}. For example, the density of the SOA examined in this study varied by approximately 30% from 1.12 to 1.49 g cm^{-3}, whereas the variation of κ_{org} is more than a factor of 2, from 0.07 to 0.16. Given the relatively narrow range of SOA density, the increasing κ_{org} with O:C suggests a negative correlation between the molecular weight and O:C for secondary organic species.

5. Discussion in the Supplemental Information:

There are a couple of topics that were fully discussed in the Supplemental Information that would better serve the reader in the main text. I suggest moving some of SI part 6 on liquid-liquid phase separation into the main text either in the introduction or section 3.3 – 3.4. In addition, the authors could add some of the Monte Carlo error assessment to the main text as well.

The simulations of the solubility distributions in the SI are quite informative. I suggest bringing some of that information into the main text or into Figure 2.

We thank the reviewer for this suggestion. We moved the discussion in SI part 6 on LLPS into section 3.3 of the main text. The section on uncertainty assessment is also moved to the main text. We left the simulations of the solubility distributions in the SI because first adding more information to Figure 2 likely will make it too busy. Second, the simulations based on a distribution of solubilities show similar trend of κ_{org} with increasing x_{AS} exhibited in the Figure 2 of the main text.

Specific comments

1) Page 2 Lines 7, 12, 18, 19: Is it hygroscopicity or is it hygroscopicity parameter?

We think it is appropriate to use “hygroscopicity” here.

2) Page 2 Line 12: Add the following…not limited by solubility at CCN activation RH, but …

We have clarified this as following:

“Therefore, for droplet activation, the organic hygroscopicity is not limited by solubility, but…”

3) Page 3 Line 19: Change hygroscopicities to hygroscopicity parameters.

Done.

4) Page 4 Line 7: Change hygroscopicity to hygroscopicity parameter.

Done.

5) Page 5 Line 1: Change atmospheric to atmospherically.

Thank you. Done.

6) Page 5 Line 3: Add the following…organic hygroscopicity at CCN activation RH is not limited.

We have clarified this as following:

“Therefore, for droplet activation, the organic hygroscopicity is not limited by solubility, but is…”

7) Page 5 Line 5: This statement “hypothesized earlier” needs a citation.

Please see response to general comment #3 above. We removed the “hypothesize earlier”. The text is changed to:

“Instead of increased solubility, the increase of the organic hygroscopicity with O:C is largely because…”

8) Page 5 line 4-6 as well as Page 21 line 16-20: These statements led to some confusion as to whether the authors are referring to the size of the precursor molecule or the oxidation products. In the same vein does the title refer to the precursor or the oxidation products?

It is the size of oxidation products (i.e., secondary organic aerosol species). On the other hand, the size of precursor and the oxidation products are related. As described in the text:

“SOA formed from smaller volatile organic compound (VOC) molecules tend to have lower average molecular weight…”

9) Page 6 Line 16: Add specificity…are the dry or water free volume fractions…

Done.

10) Page 6 Line 17: Add the following…hygroscopicityies parameters of the organics

mixtures and…

Done

11) Page 7 Line 1: Add specificity to xas, is this dry or wet mixture and under what RH.

Please see response to comment # 9. It is dry volume fraction of ammonium sulfate.

12) Page 7 Line 2: What is the chamber RH?

The chamber RH is detailed in Table S1. For most of the experiments, the chamber RH was ~ 50%. However, the initial ammonium sulfate seeds and particles exiting the chamber passed through diffusion dryers and were classified under dry conditions. We have modified the sentence to:

"…where D_{p0} and D_p are the dry diameters of initial ammonium sulfate seeds (50 nm) and size-selected particles exiting the chamber, respectively."

13) Page 7 Line 3: Add the surface tension that was assumed when deriving κCCN, org.

It is stated in the text:

"the fraction of particles serving as CCN as a function of supersaturation, which was then used to derive particle hygroscopicity κ based on κ-Köhler theory…"

"The above analysis is based on κ-Köhler theory, in which the hygroscopic parameter κ is derived assuming the surface tension of water for activating droplets."

14) Page 11 Line 19: Add…miscibility limitation at supersaturated RH.

Done.

15) Page 13 Line 20: "same behavior as pure components" That statement is incorrect due to mutual solubility, see Marcolli et al., (2004). The same applies to the statement on line 21 – 22; it is not the mass that matters, but the mixing.

This refers to the 2nd case described on page 6309 in Riipinen et al., (2015), i.e., $\gamma_i Y_{i,wet}=1$. As water condenses and particles grow, before species *i* is completely dissolved, the chemical potential of species *i* in the undissolved phase (e.g., organic phase) is same as that in the aqueous phase. If all species are non-interacting solids, then the chemical potential of species *i* in the undissolved phase is the same as pure compound, and the dissolution behavior is the same as if no other species are present (i.e., non-interacting). If the species form a solution in the undissolved phase, the mixing reduces the chemical potential of species in the undissolved phase, which translates into lower chemical potential of species in the aqueous phase (i.e., dissolved phase) and therefore reduced effective water solubility.

We clarified this in the text as follows:

For example, in a mixture of non-interacting solids, because the chemical potential of undissolved components is the same as pure compounds, the components behave independently of one another (i.e., solubility not affected by the presence of other solids, and the dissolution behavior of each species is the same as their behavior as pure components.). This is in essence the 2nd case described in Riipinen et al. (2015) (i.e., $\gamma_i Y_{i,wet}=1$).

16) Page 14 line 2: The solubility values of the pure components may not apply, but potential miscibility limitations due to liquid-liquid phase separation still applies to amorphous physical states. Please discuss. Also, by “amorphous organic state” likely “amorphous physical state” or phase state is meant.

We have clarified this in the text and changed “amorphous organic state” to “amorphous phase state”.

“We note that potential miscibility limitations due to LLPS could still apply to an amorphous phase state.”

17) Page 14 line 6 and line 8: Add comma after …particle, and after Fig. 2,

Done.

18) Page 14, line 22: A narrow density is true, but molar volume (Morg/ρorg) is used in Eq. 2, and molar volume does vary. A statement on the relative impact that Morg and ρorg have on molar volume would provide a stronger justification here.

A following statement is included:

As shown by Kuwata et al. (2013), the variation of organic density with O:C is relatively weak and can't explain the variation in κ_{org}. For example, the density of the SOA examined in this study varied by approximately 30% from 1.12 to 1.49 g cm^{-3}, whereas the variation of κ_{org} is more than a factor of 2, from 0.07 to 0.16.

19) Page 17 line 8: "non-ideal solution effects are negligible" Are they negligible? A justification is needed.

The assumption is used to estimate the molecular weight, which is around 130-160 g mol^{-1}. Given the estimated range of molecular weight and that we are discussing droplet activation (i.e., water dilution is high), this assumption is appropriate. We have rephrased the sentence to:

The above estimate assumes organics are completely dissolved (i.e., κ_{org}=$\kappa_{org,\ intr}$) and that non-ideal solution effects are negligible at the point of activation.

20) Page 18 line 3: Add…due to Eq. 2, their lower…

We rephrased the sentence to:

In essence, to have sufficiently low volatility and contribute substantially to SOA, smaller organic molecules, which have higher κ_{org} values due to their lower molecular weight based on Eq. 2, need to be more oxidized (i.e., higher O:C).

21) Page 18 line 6: Change hygroscopicity to hygroscopicity parameter.

Done.

22) Page 18 Eq 3: Use log10

Done.

23) Page 18 line 12: Jargon used; specify that this is the number of atoms.

Done

24) Page 19 Line 11: Add…leading to a lower hygroscopicity parameter via Eq. 2.

Done.

25) Page 19 line 13: Change volatility to volatilities.

Done.

26) Page 19 line 14: Use log10

Done.

27) Page 19 line 21 & 20: Change hygroscopicity to hygroscopicity parameter.

Done.

28) Page 19 line 21: Add…during the recent…

Done.

29) Page 20 line 5: Add "at CCN activation, i.e. supersaturated conditions."

Done.

30) Page 21 line 5: Change oxidize to oxidized

Done.

31) Page 21 line 11: Change hygroscopicity to hygroscopicity parameter

Done.

32) Page 21 line 13: Add… at CCN activation is controlled by…

Done.

33) Page 21 line 14: “mainly by the molecular weight of the organic species” This is the case for SOA due to the gas–particle partitioning affecting O:C and molar mass simultaneously. That concept should be added.

The concept is described in the manuscript as following:

“…due to gas-particle partitioning, SOA formed from smaller parent VOC molecules tend to have lower molecular weight and are more oxidized…”

34) Page 25 caption: …50 nm dry diameter ammonium…

…hygroscopicity parameter at high RH? is shown as a function of dry particle sulfate…

Done.

35) Figure 4 needs clarification in the x-axis label or caption that it is the carbon number of the SOA products.

Clarified.

36) The paper’s title alongside Figure 5 is confusing and needs clarification. Given the title of the paper, why is the exact opposite shown in Figure 5, i.e., increasing O:C with increasing κCCN, org. Why not plot molecular weight vs. κCCN, org? Then the spread in the data would be the O:C dependence, which would reflect the main point of the paper.

We thank the referee for this suggestion. However, molecular weight of organic species was not directly measured in these experiments, and Lambe et al (2011) did not report the relationship between κ_{org} and molecular weight (for the same reason). The main purpose of the figure is to demonstrate that the model, which is based on the absence of solubility limitation of κ_{org}, can successfully produce the observed relationship between κ_{org} and O:C.

References

Bilde, M., Svenningsson, B., Mønster, J. and Rosenørn, T.: Even-odd alternation of evaporation rates and vapor pressures of C3-C9 dicarboxylic acid aerosols, Environ. Sci. Technol., doi:10.1021/es0201810, 2003.

Kuwata, M., Shao, W., Lebouteiller, R. and Martin, S. T.: Classifying organic materials by oxygen-to-carbon elemental ratio to predict the activation regime of Cloud Condensation Nuclei (CCN), Atmos. Chem. Phys., 13(10), 5309–5324, doi:10.5194/acp- 13-5309-2013, 2013.

Marcolli, C., Luo, B. and Peter, T.: Mixing of the Organic Aerosol Fractions: Liquids as the Thermodynamically Stable Phases, J. Phys. Chem. A, doi:10.1021/jp036080l, 2004.

Ovadnevaite, J., Zuend, A., Laaksonen, A., Sanchez, K. J., Roberts, G., Ceburnis, D., Decesari, S., Rinaldi, M., Hodas, N., Facchini, M. C., Seinfeld, J. H. and O' Dowd, C.: Surface tension prevails over solute effect in organic-influenced cloud droplet activation, Nature, 546(7660), 637–641, doi:10.1038/nature22806, 2017.

Petters, M. D. and Kreidenweis, S. M.: A single parameter representation of hygroscopic growth and cloud condensation nucleus activity – Part 2: Including solubility, Atmos.

Chem. Phys., 7(8), 1961–1971, doi:10.5194/acp-7-1961-2007, 2007.

Petters, M. D., Kreidenweis, S. M., Prenni, A. J., Sullivan, R. C., Carrico, C. M., Koehler,

K. A. and Ziemann, P. J.: Role of molecular size in cloud droplet activation, Geophys. Res. Lett., 36(22), 1–5, doi:10.1029/2009GL040131, 2009.

Petters, M. D., Kreidenweis, S. M. and Ziemann, P. J.: Prediction of cloud condensation nuclei activity for organic compounds using functional group contribution methods, Geosci. Model Dev., 9(1), 111–124, doi:10.5194/gmd-9-111-2016, 2016.

Rastak, N., Pajunoja, A., Acosta Navarro, J. C., Ma, J., Song, M., Partridge, D. G., Kirkevåg, A., Leong, Y., Hu, W. W., Taylor, N. F., Lambe, A., Cerully, K., Bougiatioti, A., Liu, P., Krejci, R., Petäjä, T., Percival, C., Davidovits, P., Worsnop, D. R., Ekman, A.

M. L., Nenes, A., Martin, S., Jimenez, J. L., Collins, D. R., Topping, D. O., Bertram, A. K., Zuend, A., Virtanen, A. and Riipinen, I.: Microphysical explanation of the RH- dependent water affinity of biogenic organic aerosol and its importance for climate, Geophys. Res. Lett., 44(10), 5167–5177, doi:10.1002/2017GL073056, 2017.

Renbaum-Wolff, L., Song, M., Marcolli, C., Zhang, Y., Liu, P. F., Grayson, J. W., Geiger,

F. M., Martin, S. T. and Bertram, A. K.: Observations and implications of liquid–liquid phase separation at high relative humidities in secondary organic material produced by α-pinene ozonolysis without inorganic salts, Atmos. Chem. Phys., 16(12), 7969–7979, doi:10.5194/acp-16-7969-2016, 2016.

Riipinen, I., Rastak, N. and Pandis, S. N.: Connecting the solubility and CCN activation of complex organic aerosols: A theoretical study using solubility distributions, Atmos. Chem. Phys., 15(11), 6305–6322, doi:10.5194/acp-15-6305-2015, 2015.

Sullivan, R. C., Moore, M. J. K., Petters, M. D., Kreidenweis, S. M., Roberts, G. C. and Prather, K. A.: Effect of chemical mixing state on the hygroscopicity and cloud nucleation properties of

calcium mineral dust particles, Atmos. Chem. Phys., 9(10), 3303–3316, doi:10.5194/acp-9-3303-2009, 2009.

We thank the referees for their constructive comments. Please find below detailed responses to each comment or question, including notations of improvements to the manuscript. Referee comments are in blue fonts. Changes to the text are highlighted in yellow.

Referees' comments:

Anonymous Referee #2

Received and published: 5 September 2018

Cloud droplet activation of organic compounds depends on various parameters such as solubility, molecular weight, density, and surface activity. A large number of studies have investigated the role of different parameters in cloud droplet activation using pure compounds or simple mixtures. However, since atmospheric organic aerosols are comprised of numerous unknown compounds, it remains to be challenging to understand controlling parameters in cloud droplet activation of organic aerosol. Empirical relationships between the hygroscopicity parameter kappa and O/C have been widely used to infer the effects of aging of organic aerosol on CCN activity. However, underlying mechanisms of the relationship remain uncertain. In this paper, they performed smog chamber experiments to study the role of solubility in cloud droplet activation.

In their experiments, size-selected ammonium sulfate particles were introduced into a smog chamber and varying amount of SOA was condensed according to different residence time distribution in the steady-state chamber. By analyzing the hygroscopicity parameter kappa at different diameter (and supersaturation), they evaluated the dependence of apparent organic kappa as a function of ammonium sulfate (AS) fraction that affects the amount of liquid water at the point of activation. They found that for the majority of chamber-generated SOA (except for beta-caryophyllene SOA), there was no significant dependence of apparent kappa of organics on AS fraction, suggesting that solubility-limitation is largely absent in those SOA investigated in this study. They further performed model calculations to show that apparent linear dependence of kappa of organics and O/C is primarily due to molecular weight. The experiments were carefully performed and the paper is well written. However, I would like to see more careful citations of literature to put this study into a better context. The following are specific comments.

1) The introduction gives an impression that previous study assumed solubility of SOA compounds is the only controlling parameter (although it may not be the authors' intent). Jimenez et al. (2009), Riipinen et al. (2015), and Nakao (2017) are cited as examples of studies that hypothesized that increase in solubility leads to increase in kappa (p.4 L9-19).

a. I believe Jimenez et al. only showed a correlation between kappa and O/C without proposing a mechanism.

b. Riipinen et al. showed that distribution of solubility in the range of 0.1 – 100 g L-1 (or 1e-4 to 1e-1 in volume scale if a unit density is assumed) is critical for capturing the CCN activation. Riipinen et al. recognized that some SOA are sufficiently soluble: “. . .the observations of the close-to-complete dissolution of SOA at activation (Huff Hartz et al., 2005; Engelhart et al., 2008) indicate that the majority of the material in the studied SOA mixtures had solubilities larger than 10 g L-1.”

c. Nakao investigated the combined role of solubility and molar volume through the 2D-VBS framework (C* vs O/C): “The model calculation provides a plausible explanation on why O/C can have an impact on k. The mechanism is likely to be not just the solubility (Kuwata et al. 2013; Riipinen et al. 2015), but a combination of the solubility and volatility that determines the molecular size of dissolved solutes.”

Therefore, both Riipinen et al. and Nakao recognized that solubility plays a role only up to a certain threshold that depends on solubility distributions. I believe the value of this study is that it experimentally showed many of SOA constituents are past that threshold.

We thank the reviewer for the comment. We have revised the introduction accordingly:

For single component aerosols and simple mixtures, the effect of increasing oxidation level on water solubility and in turn hygroscopicity is well established (Petters et al., 2009;Petters et al., 2016;Rickards et al., 2013;Kuwata et al., 2013). Water solubility is defined as the amount solute that can dissolve in water at saturation, corresponding to solid/aqueous solution equilibrium. Miscibility is related to solubility and refers to the ability of two liquid phases to mix. Miscibility limitation leads to liquid-liquid phase separation (LLPS). If LLPS occurs under supersaturated conditions, miscibility can exert similar control on droplet activation as water solubility (Petters et al., 2006;Petters et al., 2016), and is further discussed in a later section. Kuwata et al. (2013) shows that for single organic compounds, water solubility generally increases with O:C. One plausible explanation is that as organic molecules become increasingly oxidized (i.e., increased O:C ratio), they are more polar, leading to increased water solubility. As O:C increases from near zero, the regime for the activation of single organic compound transitions from insoluble, to slightly soluble, then to highly soluble, leading to a general increasing trend of hygroscopicity parameter (Kuwata et al., 2013). In the highly soluble regime, the hygroscopicity parameter is no longer limited by water solubility, but controlled mainly by molecular weight instead (e.g., Kuwata et al., 2013). Nakao (2017) modeled the hygroscopicity of secondary organic species, and the results suggest the increase of organic hygroscopicity with O:C is likely due to a combination of both increased water solubility and variation in volatility that determines the molecular size of dissolved solute. Riipinen et al. (2015) examined cloud activation of multicomponent organic particles theoretically and suggested that the organic hygroscopicity parameter is strongly influenced by the distributions of species with water solubility between 0.1 and 100 g L^{-1}, i.e., the range for slightly soluble species. Whereas all the above studies suggest that the hygroscopicity parameter is strongly influenced by water solubility of slightly soluble organics, for ambient organic aerosols and laboratory generated secondary organic aerosols, the influence of water solubility on organic hygroscopicity has not been systematically examined experimentally, and the underlying mechanism for the increasing hygroscopicity with increasing O:C remains unclear.

2) Kuwata et al. (2013) is cited as an example of studies on pure species, but they did also investigate alpha-pinene SOA and isoprene SOA. Isoprene SOA was found to be highly soluble. Alpha-pinene SOA was predicted to be slightly soluble based on O/C alone but observed to be highly soluble. They hypothesized that the amorphous state of organics led to continuous water uptake without deliquescence. More discussion is needed in assessing the consistency with Kuwata et al. (2013).

We have added the comparison with κ_{org} of isoprene and α-pinene SOA reported by Kuwata et al. (2013). In addition, we now included the reference of Kuwata et al. (2013) when discussing the amorphous state of organics. The texts are changed to:

The constant κ_{org} with x_{AS} for isoprene SOA agrees with the results from an earlier study (King et al., 2010), and the κ_{org} values for isoprene and α-pinene SOA are consistent with the values reported in earlier studies (e.g., Kuwata et al., 2013).

Upon humidification of the amorphous particle in a metastable state, sparingly soluble compounds can freely partition into the liquid phase, and water uptake is continuous without the first order phase transition (e.g., Kuwata et al., 2013).

3) Consistency with the solubility parameterization developed by Kuwata et al. (2013), $\ln C = 20*[(O/C)\hat{}0.402 - 1]$, needs to be evaluated. Can the observation be reproduced using measured O/C values in this study? For instance, using beta-caryophyllene's measured O/C = 0.33, C is calculated to be 7.5e-4. Based on Figure S7, it seems the wider distribution case is consistent with the experiment. A discussion along this line would be helpful.

We thank the reviewer for this suggestion. Based on the O:C value of 0.33, the solubility of β-caryophyllene SOA is estimated as 7.5e-4 (Kuwata et al. 2013). The measured variation of κ_{org}

with x_{AS} β-caryophyllene SOA is broadly consistent with the simulated trend for mixtures with a distribution of water solubilities shown in Fig. S7. This discussion is included in the revision.

“It is also worth noting that based on the O:C value of 0.33, the solubility of β-caryophyllene SOA is estimated as 7.5×10^{-4} (Kuwata et al. 2013). The measured variation of κ_{org} with x_{AS} for β-caryophyllene SOA is broadly consistent with the simulated trend for mixtures with a distribution of water solubilities shown in Fig. S7.”

4) There can be a number of exceptions to the title. More careful clarification of poten- tial exceptions should be discussed, or the title needs to be reconsidered. Within their experiments, beta-caryophyllene SOA is controlled by solubility up to AS 15%. They use toluene as an example of the major precursors of anthropogenic SOA. I would ex- pect SOA produced from large alkanes (linear, branched, cyclic) potentially important in the urban atmosphere (Gentner et al. 2017) would be solubility limited. It remains unknown whether SOA formed from larger aromatic hydrocarbons such as trimethyl- benzene, naphthalene, and methylnaphthalenes are solubility-limited.

We agree that there can be exceptions, and we have included the following discussion in the revision.

We note there can be exceptions to this finding. Whereas on the global scale, SOA is dominated by those formed from isoprene, monoterpene, and small aromatic hydrocarbons such as toluene, SOA produced from large alkanes and aromatics are potentially important in the urban atmosphere (Gentner et al. 2017), and their droplet activation may be limited by organic water solubility, especially when the volume fraction of inorganics in the particles is low.

5) What are the potential impacts of nitrogen and sulfur-containing organics? Suda et al. showed that nitrates are less CCN active (Suda et al. 2014).

The experiments were carried out in a range of NO concentrations. We expect the organic nitrates formed in these experiments are broadly representative of those in the ambient. Whereas organic nitrates are generally less CCN active, results from our experiments indicate that nearly all organics are dissolved at the point of activation. This may be because (1) other functional groups present in the same organic nitrate molecules overcame the solubility/miscibility limitations and/or (2) the presence of water-soluble organics facilitates the solvation of the less water-soluble species such as organic nitrates. We expect that production of sulfur-containing organics was suppressed in our experiments due to the chamber conditions (i.e., dry ammonium sulfate seeds were used, and the seeds were fully neutralized). We are not aware of any work on the hygroscopicity of typical sulfur-containing secondary organic species. We speculate that organosulfates are more polar compounds and their droplet activation is probably not limited by water solubility.

References

Gentner, D. R., Jathar, S. H., Gordon, T. D., Bahreini, R., Day, D. A., El Haddad, I.,

Hayes, P. L., Pieber, S. M., Platt, S. M., de Gouw, J., Goldstein, A. H., Harley, R. A., Jimenez, J. L., Prévôt, A. S. H., Robinson, A. L. (2017). Review of Urban Secondary Organic Aerosol Formation from Gasoline and Diesel Motor Vehicle Emissions. Envi- ronmental Science & Technology 51:1074-1093.

Suda, S. R., Petters, M. D., Yeh, G. K., Strollo, C., Matsunaga, A., Faulhaber, A., Ziemann, P. J., Prenni, A. J., Carrico, C. M., Sullivan, R. C., Kreidenweis, S. M. (2014). Influence of Functional Groups on Organic Aerosol Cloud Condensation Nucleus Ac- tivity. Environmental Science & Technology 48:10182-10190.

Cloud droplet activation of secondary organic aerosol is mainly controlled by molecular weight, not water solubility

Jian Wang[1,2], John E. Shilling[3~~2~~], Jiumeng Liu[3~~2~~,4~~3~~], Alla Zelenyuk[5~~4~~], David M. Bell[5~~4~~,6~~5~~], Markus Petters[7~~6~~], Ryan Thalman[1,8~~7~~], Fan Mei[3~~2~~], Rahul A. Zaveri[3~~2~~], and Guangjie Zheng[1,2]

[1]Environmental and Climate Sciences Department, Brookhaven National Laboratory, Upton, New York 11973, USA

[2]Center for Aerosol Science and Engineering, Department of Energy, Environmental and Chemical Engineering, Washington University in St. Louis, Missouri, USA

[~~2~~3]Atmospheric Sciences and Global Change Division, Pacific Northwest National Laboratory, Richland, Washington 99354, USA

[~~3~~4]Present address: School of Environment, Harbin Institute of Technology, Harbin, China 150001

[5~~4~~]Physical Sciences Division, Pacific Northwest National Laboratory, Richland, Washington 99354, United States

[6~~5~~]Present address: Laboratory of Atmospheric Chemistry, Paul Scherrer Institute, 5232 Villigen-PSI, Switzerland

[7~~6~~]Department of Marine, Earth, and Atmospheric Sciences, North Carolina State University at Raleigh, Raleigh, North Carolina 27695, USA

[8~~7~~]Present address: Department of Chemistry, Snow College, Richfield, Utah 84627, USA

Correspondence to: Jian Wang (jian@wustl.edu~~bnl.gov~~)

Abstract

Aerosol particles strongly influence global climate by modifying the properties of clouds. An accurate assessment of the aerosol impact on climate requires knowledge of the concentration of cloud condensation nuclei (CCN), a subset of aerosol particles that can activate and form cloud droplets in the atmosphere. Atmospheric particles typically consist of a myriad of organic species, which frequently dominate the particle composition. As a result, CCN concentration is often a strong function of the hygroscopicity of organics in the particles. Earlier studies showed organic hygroscopicity increases nearly linearly with oxidation level. Such increase of hygroscopicity is conventionally attributed to higher water solubility for more oxidized organics. By systematically varying the water content of activating droplets, we show that for the majority of secondary organic aerosols (SOA), essentially all organics are dissolved at the point of droplet activation. Therefore, for droplet activation, the organic hygroscopicity is not limited by solubility, but is dictated mainly by the molecular weight of organic species. Instead of increased water solubility as previously thought, the increase of the organic hygroscopicity with oxidation level is largely because (1) SOA formed from smaller precursor molecules tend to be more oxidized and have lower average molecular weight and (2) during oxidation, fragmentation reactions reduce average organic molecule weight, leading to increased hygroscopicity. A simple model of organic hygroscopicity based on molecular weight, oxidation level, and volatility is developed, and it successfully reproduces the variation of SOA hygroscopicity with oxidation level observed in the laboratory and field studies.

1. Introduction

A prerequisite for cloud formation, aerosol particles strongly impact global climate by influencing the properties of clouds (Twomey, 1977;Albrecht, 1989). These effects, named aerosol indirect effects, represent one of the largest uncertainties in the simulated change of global radiation fluxes (i.e., radiative forcing) due to the increase of aerosol concentration since pre-industrial era (IPCC, 2013). An accurate assessment of the aerosol indirect effects requires the knowledge of the concentration of cloud condensation nuclei (CCN), a subset of aerosol particles that can activate and form cloud droplets in the atmosphere. The efficiency with which particles activate and transform into cloud droplets depends on particle size and hygroscopicity parameter κ (Petters and Kreidenweis, 2007), which combines a number of thermodynamic properties of the species within the particles to describe the tendency of the particles to uptake water ~~(Petters and Kreidenweis, 2007)~~. It is worth noting that the value of hygroscopicity parameter κ may vary with relative humidity. The κ values examined in this study are at droplet activation under supersaturated conditions, and they may be different from those under sub-saturated conditions associated with particle hygroscopic growth.

The inorganic fraction of atmospheric aerosol particles typically consists of a very limited number of species, e.g., sulfate and nitrate, whose hygroscopicities are well studied (Petters and Kreidenweis, 2007). However, atmospheric particles often consist in addition to inorganic species, of hundreds, or even thousands of organic species (Zhang et al., 2007). Collectively, these organic species often dominate the composition of sub-micrometer aerosol particles, which represent the majority of CCN population. These organic species in ambient particles have a wide range of hygroscopicity parameters~~ies~~, from zero for hydrophobic organics to as high as 0.3 for some of the water soluble organics (e.g., Petters et al., 2009;Moore et al., 2012;Lathem et al., 2013). Modeling studies show that CCN concentrations can be a strong function of the hygroscopicity of organics in the particles (e.g., McFiggans et al., 2006;Mei et al., 2013). This is particularly true for modeling cloud formation during pre-industrial era, when organics represented an even larger fraction of the submicron aerosol mass concentration due to the low concentration of anthropogenic sulfate (Mei et al., 2013;Liu and Wang, 2010). Neglecting the variation of the organic hygroscopicity may lead to substantial bias in modeled aerosol indirect forcing, which represents a change in radiation flux due to the increased aerosol concentration since pre-industrial era (Liu and Wang, 2010).

Several studies show that for ambient organic aerosols and laboratory generated secondary organic aerosols (SOA), organic hygroscopicity parameter increases nearly linearly with the atomic O:C ratio (e.g., Jimenez et al., 2009;Lambe et al., 2011), a parameter commonly used to quantify oxidation level of organics. For single component aerosols and simple mixtures, the effect of increasing oxidation level on water solubility and in turn hygroscopicity is well established (Petters et al., 2009;Petters et al., 2016;Rickards et al., 2013;Kuwata et al., 2013). Water solubility is defined as the amount solute that can dissolve in water at saturation, corresponding to solid/aqueous solution equilibrium. Miscibility is related to solubility and refers to the ability of two liquid phases to mix. Miscibility limitation leads to liquid-liquid phase separation (LLPS). If LLPS occurs under supersaturated conditions, miscibility can exert similar control on droplet activation as water solubility (Petters et al., 2006;Petters et al., 2016), and is further discussed in a later section. Kuwata et al. (2013) shows that for single organic compounds, water solubility generally increases with O:C. One plausible explanation is that as organic molecules become increasingly oxidized (i.e., increased O:C ratio), they are more polar, leading to increased water solubility. As O:C increases from near zero, the regime for the activation of single organic compound transitions from insoluble, to slightly soluble, then to highly soluble, leading to a general increasing trend of hygroscopicity parameter (Kuwata et al., 2013). In the highly soluble regime, the hygroscopicity parameter is no longer limited by water solubility, but controlled mainly by molecular weight instead (e.g., Kuwata et al., 2013). Nakao (2017) modeled the hygroscopicity of secondary organic species, and the results suggest the increase of organic hygroscopicity with O:C is likely due to a combination of both increased water solubility and variation in volatility that determines the molecular size of dissolved solute. Riipinen et al. (2015) examined cloud activation of multicomponent organic particles theoretically and suggested that the organic hygroscopicity parameter is strongly influenced by the distributions of species with water solubility between 0.1 and 100 g L^{-1}, i.e., the range for slightly soluble species. Whereas all the above studies suggest that the hygroscopicity parameter is strongly influenced by water solubility of slightly soluble organics, for ambient organic aerosols and laboratory generated secondary organic aerosols, the influence of water solubility on organic hygroscopicity has not been systematically examined experimentally, and the underlying mechanism for the increasing hygroscopicity with increasing O:C remains unclear. ~~It has long been hypothesized that as organic molecules become increasingly oxidized (i.e., increased O:C ratio), they are more polar, leading to increased water solubility and therefore hygroscopicity (Jimenez et al., 2009;Riipinen et al., 2015). Nakao (2017) modeled the impact of volatility and water solubility on the hygroscopicity of secondary organic species, and also attributed the increase of organic hygroscopicity with O:C to an increased solubility for more oxidized organics.~~ ~~For single component aerosols and simple mixtures, the effect of increasing oxidation level on solubility and in turn hygroscopicity is well established (Kuwata et al., 2013; Petters et al., 2009; Petters et al., 2016; Rickards et al., 2013).~~ ~~However, the hypothesis, namely~~

~~that the increase of organic hygroscopicity with oxidation level for ambient organic aerosols and laboratory generated secondary organic aerosols is due to increased water solubility, has not been tested experimentally.~~ In this study, we designed and carried out experiments to explicitly examine the mechanism by which changes in O:C ratio lead to variations in organic hygroscopicity. This wa~~i~~s achieved by systematically varying the water content of activating droplets to examine the impact of water solubility on the effective hygroscopicity of secondary organic aerosols, which were generated in an environmental chamber from representative precursors under a range of atmospherically relevant conditions. We show that for many secondary organic aerosols (SOA), essentially all organics are dissolved at the point of activation. Therefore, for droplet activation, organic hygroscopicity is not limited by solubility, but is controlled mainly by the molecular weight of organic species in particles. Instead of increased solubility~~ as hypothesized earlier~~, the increase of the organic hygroscopicity with O:C is largely because (a) SOA formed from smaller volatile organic compound (VOC) molecules tend to have lower average molecular weight and higher O:C and (b) during oxidation, fragmentation reactions lead to smaller organic molecules with lower molecular weight and higher O:C.

2. Methods

2.1 Experiments

Secondary organic aerosols were generated in a steady state environmental chamber (Shilling et al., 2008) from representative VOC, including isoprene, α-pinene, Δ-3 carene, β-caryophyllene, and toluene. Dry ammonium sulfate particles of 50 nm were classified by a

Differential Mobility Analyzer (DMA), and introduced as seed particles along with the VOC into the chamber. The reaction of the VOC with oxidants led to formation of secondary organic species, which condensed on the ammonium sulfate seed particles, leading to particle growth. No new particle formation was observed during the experiments. The experimental setup and conditions are detailed in the Supplementary Information. Given the distribution of particle residence time inside the steady state chamber, particles exit the chamber with a range of particle sizes (Shilling et al., 2008), and hence sulfate volume fractions. The particles were sampled by a size-resolved CCN system (Mei et al., 2013), in which they were first size selected by a DMA. The total number and CCN concentrations of the size-selected particles were simultaneously measured by a condensation particle counter and a CCN counter, respectively. These measured number concentrations yielded the activation spectrum, i.e., the fraction of particles serving as CCN as a function of supersaturation, which was then used to derive particle hygroscopicity κ based on κ-Köhler theory (Mei et al., 2013;Petters and Kreidenweis, 2007). Given that all particles were grown on seed particles of essentially the same diameter, the hygroscopicities of SOA particles with different sulfate volume fractions were characterized by size selecting particles of different final diameters.

2.2 Derivation of effective organic hygroscopicity

Because no new particle formation was observed, and measured particles were larger than the initial seed particle size, particles exiting the chamber are assumed as internal mixture (i.e., at any given size, particles of same diameter have essentially the same composition). For internal mixtures, particle hygroscopicity κ is given by the volume average of participating species (Petters and Kreidenweis, 2007):

$$\kappa = x_{\mathrm{org}}\kappa_{\mathrm{org}} + x_{\mathrm{AS}}\kappa_{\mathrm{AS}} = (1 - x_{\mathrm{AS}})\kappa_{\mathrm{org}} + x_{\mathrm{AS}}\kappa_{\mathrm{AS}} \qquad (1)$$

where x_{org} and x_{AS} are the dry volume fractions of organics and ammonium sulfate, respectively, and κ_{org} and κ_{AS} are the ~~hygroscopicities~~ hygroscopicity parameters of the organics and ammonium sulfate (0.61), respectively. Eq. 1 implies an ideal Zdanovskii, Stokes, and Robinson (ZSR) mixing. We note that κ_{org} represents the apparent organic hygroscopicity (Sullivan et al., 2009), also referred to as the effective hygroscopicity (Pringle et al., 2010). This effective hygroscopicity includes the overall impact of the organics on particle activation, including water solubility (Sullivan et al., 2009). The value of x_{AS} is given by $\left(D_{\mathrm{p0}}/D_{\mathrm{p}}\right)^3$, where D_{p0} and D_{p} are the dry diameters of initial ammonium sulfate seeds (50 nm) and size-selected particles exiting the chamber, respectively. The value of κ_{org} can then be derived from measured particle hygroscopicity κ and sulfate volume fraction x_{AS} using Eq. 1. A small fraction of the seeds was doubly charged and had diameters larger than 50 nm. For the derivation of κ_{org}, particles grown from doubly charged seeds are taken into consideration using an approach described in the Supplementary Information.

2.3 Uncertainty of derived effective organic hygroscopicity

As organic particles formed by condensational growth of ammonium sulfate seeds are spherical (Zelenyuk et al., 2008), no shape factor correction is necessary for the derivation of particle κ from the measured particles sizes. The impact of coagulation is minor under the experimental conditions. The value of κ_{org} was derived from Eq. 1, therefore its uncertainty derives from the uncertainties of particle κ and sulfate volume fraction. As particle κ was derived from the activation spectrum (the variation of activated fraction as a function of supersaturation) of size-selected particles, the uncertainty in particle κ can be attributed to the uncertainties in particles size, supersaturation of CCN counter, and activation fractions. The uncertainty in sulfate volume fraction derives from the uncertainties in the mode diameters of ammonium sulfate seeds and grown particles size-selected for CCN measurements.

Given the steps involved in the derivation of κ_{org}, it is difficult to obtain the uncertainty of κ_{org} analytically through error propagation. Instead, the uncertainty was calculated numerically using a Monte Carlo approach described as follows. The CCN counter supersaturation, activation fraction, and the mode diameters of ammonium sulfate seeds and grown particles size-selected for CCN measurements were randomly chosen from normal distributions with respective mean values and standard deviations. These randomly chosen parameters were then used to calculate κ_{org} following the method described above. The above calculation was repeated 100 times, and the uncertainty of κ_{org} was derived from the distribution of the 100 κ_{org} values. The distribution of CCN counter supersaturation was assumed as a normal distribution, and the mean and standard deviation of the distribution was derived from the repeated calibration values. The mode diameter of ammonium sulfate seeds, the mode diameter of grown particles size-selected for CCN measurements, and the activated fraction were assumed to have normal distributions with standard deviations as 1%, 1%, and 5% of the mean values, respectively.

3. Results and Discussions

3.1 Effective organic hygroscopicity for secondary organic aerosols formed on sulfate seeds

The effective organic hygroscopicity κ_{org} was derived from the overall κ of particles for a range of final particle sizes (i.e., sulfate volume fractions). The variation of κ_{org} with x_{AS} is shown in Fig. 1 for SOA formed from representative VOC precursors, including isoprene, α-pinene, β-caryophyllene, and toluene. We note that isoprene is the most abundant non-methane hydrocarbon, α-pinene and β-caryophyllene are the most abundant natural monoterpene and sesquiterpene species globally, and toluene is a representative anthropogenic SOA precursor (Pye et al., 2010;Guenther et al., 2012). The uncertainty of the derived κ_{org} was estimated using a Monte Carlo method based on the uncertainties in the CCN counter supersaturation, measured activated fraction, and mode diameters of size-selected particles and the ammonium sulfate seeds (see Supplementary Information for details). Figure 1 shows that κ_{org} is essentially independent of x_{AS} for SOA formed from isoprene, α-pinene, and toluene, while it decreases with decreasing x_{AS} below 15% for SOA formed from β-caryophyllene. The constant κ_{org} with x_{AS} for isoprene SOA agrees with the results from an earlier study (King et al., 2010), and the κ_{org} values for isoprene and α-pinene SOA are consistent with the values reported in earlier studies (e.g., Kuwata et al., 2013). ~~.~~The effective organic hygroscopicity and its variation with x_{AS} were also examined for SOA formed from α-pinene and Δ-3 carene under a variety of conditions (Figure S1, details given in Supplementary Information). ~~Again~~Again, the results show that κ_{org} is essentially independent of x_{AS}. A nearly constant κ_{org} indicates that cloud droplet activation of the particles is not limited by organic water solubility, because otherwise, we would have observed a dependence on x_{AS} as explained below.

3.2 Effect of water solubility on droplet activation of organic particles

Following the same definition as in Sullivan et al. (2009), we introduce the intrinsic hygroscopicity $\kappa_{org,\ intr}$, which represents the organic hygroscopicity if a compound is fully dissolved at the point of the activation (i.e., peak of the Köhler curve). The intrinsic hygroscopicity parameter of a compound at droplet activation can be estimated from (Sullivan et al., 2009):

$$\kappa_{org,\mathrm{int}r} = \frac{i\rho_{org}M_w}{\rho_w M_{org}} \quad (2)$$

Where ρ is the density, M is the molecular weight, and i is the van't Hoff factor. The subscripts "org" and "w" represent organics and water, respectively. If the organic species are completely dissolved at the point of activation, the values of κ_{org} and $\kappa_{\mathrm{org,\ intr}}$ are equal. For particles consisting of compounds with limited solubility, κ_{org} may exhibit a lower value than $\kappa_{\mathrm{org,\ intr}}$.

Figure 2 shows the effective organic hygroscopicity κ_{org} simulated for particles composed of ammonium sulfate seed and a model organic compound with $\kappa_{\mathrm{org,\ intr}}$ of 0.15. Same as the particles sampled during the experiments, modelled particles are assumed to have a sulfate core with a diameter of 50 nm. The value of κ_{org} was simulated for particles with different organic coating thicknesses and therefore x_{AS}. The simulation was carried out for a range of organic water solubility C, from 5×10^{-2} (i.e., moderately soluble) to 1×10^{-5} (i.e., effectively insoluble, Petters and Kreidenweis, 2008). Here the solubility C is defined as the volume of compound per unit volume of water (Petters and Kreidenweis, 2008). For organics with C of 1×10^{-2} or lower (sparingly soluble species), simulated κ_{org} exhibits a value close to zero at 1% x_{AS} due to the limitation of solubility. The κ_{org} value increases with increasing x_{AS}, and eventually reaching a plateau at the intrinsic $\kappa_{\mathrm{org,\ intr}}$ (i.e., 0.15), at which point droplet activation is no longer limited by organics solubility. Sparingly soluble organics with higher C reaches the plateau at lower x_{AS}. When $C \geq 5\times10^{-2}$, the effective organic hygroscopicity κ_{org} is 0.15 at all x_{AS} values, indicating the organic compound becomes completely dissolved at the point of activation and droplet activation is not limited by organic solubility even for "pure" organic particles (i.e., x_{AS}=0%). This is consistent with the classification scheme that divides the aerosol in effectively soluble, sparingly soluble, and effectively insoluble (Petters and Kreidenweis, 2008). For $10^{-4} < C < 0.05$, the organic compound is sparingly soluble and x_{AS} controls the value of κ_{org}. This is because the water uptake by ammonium sulfate increases the amount of water in the growing droplet that is available for solvation of organics. Examples of the Köhler curve for the mixtures are shown in the Supplementary Information (Fig. S6). Even for compounds with a very low solubility of 10^{-4} that are effectively insoluble when considering “pure” organic particles, they are completely dissolved at the point of activation for mixtures with ~96% or more sulfate by volume. Atmospheric organic aerosols consist of many components with different solubilities. If the model is initialized with a distribution of solubilities (Riipinen et al., 2015 and Supplementary Information) that are centered at the same values as those shown in Fig. 2, the general behavior exhibited in Fig. 2 is retained, whereas the sparingly soluble range is shifted toward lower solubilities (Fig. S7).

3.3 Comparison of observed and calculated dependence of κ_{org} on sulfate volume fraction

The simulated variation of κ_{org} with x_{AS} for sparingly soluble organics above is in clear contrast to the experimental results of monoterpene, isoprene, and toluene SOA that show an essentially constant κ_{org} for a wide range of x_{AS}. The essentially constant κ_{org} is consistent with the simulated cases for more soluble organics (i.e., *C* value of 0.05 and larger), suggesting that the effective organic hygroscopicity κ_{org} is the same, or at least very close to, the intrinsic hygroscopicity $\kappa_{org,\ intr}$ for mixtures with x_{AS} as low as 3%. As ambient particles typically consist of more than 3% highly soluble species such as sulfate or nitrate by volume, this suggests that for ambient particles, most secondary organic species formed from common precursors including isoprene, α-pinene, and toluene are completely dissolved at the point of activation, therefore their hygroscopicity is not limited by water solubility. We note that SOA formed from β-caryophyllene, whose droplet activation exhibits solubility limitation when x_{AS}<15%, represents a relatively minor contribution to organic aerosol globally. In addition, most ambient aerosols consist of 15% or more highly ~~water soluble~~water-soluble inorganic species. It is also worth noting that κ_{org} of α-pinene SOA in this study is within the range of those derived from α-pinene SOA particles formed without inorganic seeds (e.g., Alfarra et al., 2013;Zhao et al., 2016), suggesting that even for some “pure SOA” particles, most organic species are dissolved at the point of activation, and the limitation of hygroscopicity by water solubility is negligible. Table 1 lists the intrinsic hygroscopicity derived using Eq. 1 for major monoterpene SOA species. Here we assume organic molecules in SOA do not dissociate when dissolved in water therefore i=1 (Ervens et al., 2005). The assumption of i=1 is valid only under conditions of high dilution in water, such as at droplet activation under supersaturated conditions. For most of these compounds, the intrinsic hygroscopicity is consistent with κ_{org} derived from α-pinene experiments, again suggesting that the droplet activation of α-pinene SOA is not limited by organic water solubility. We note that SOA may consist of substantial amount of the oligomers (Kalberer et al., 2004). It is not clear whether these oligomers dissociate in growing droplets during activation. If not, the formation of oligomers would lead to a lower κ_{org} as a result of increased molecular weight. ~~Therefore~~Therefore, the $\kappa_{org,\ intr}$ values in Table 1 likely represent an upper limit.

For SOA formed from β-caryophyllene, κ_{org} showed lower values when x_{AS} is less than 15%. This is consistent with simulated trends for sparingly soluble organics, suggesting only a fraction of organics are dissolved at the point of activation, and the droplet activation of β-caryophyllene SOA in our study is limited by the organic solubility at low x_{AS}. This may be due to lower solubility of β-caryophyllene SOA than those formed from α-pinene, Δ-3 carene, isoprene, and toluene because of the larger precursor molecule. The extrapolation of the data points suggests κ_{org} of ~ 0.03 for β-caryophyllene SOA formed without ammonium sulfate seeds, consistent with the low values (i.e., $0 \leq \kappa_{org} \leq 0.05$) reported by earlier studies (Asa-Awuku et al., 2009;Frosch et al., 2013).

We note particles may undergo liquid-liquid phase separation (LLPS) instead of a solubility transition (Bertram et al., 2011;Zuend and Seinfeld, 2012). Solubility refers to the amount of material present in the saturated solution. For an initially dry particle, solubility and water activity of the saturated solution will control the size and RH at which pure crystalline substances spontaneously dissolve (Shulman et al., 1996;Hori et al., 2003;Bilde and Svenningsson, 2004;Petters and Kreidenweis, 2008). For particles that include sparingly soluble compounds, the dissolution occurs in the supersaturated regime and thereby exerts some control over the critical supersaturation. This gives rise to strong sensitivity of κ_{org} with increasing inorganic fraction. Miscibility is related to solubility and refers to the ability of two liquid phases to mix. Substances that form two liquid phases are immiscible. If a miscibility transition occurs in the supersaturated regime, miscibility limitations exert a similar control over critical supersaturation as solubility (Petters et al., 2006;Petters et al., 2016), i.e., the effective hygroscopicity κ_{org} observed from CCN activation is reduced at lower net water contents (smaller size or less hygroscopic material present). In essence, the presence of undissolved organics can be considered as a special case of LLPS (i.e., the undissolved organics form the 2nd phase). Distinguishing between miscibility and solubility in CCN experiments is not possible because the manifestation of the effect is identical.

In general, SOA precursors are weakly oxidized hydrocarbons. These hydrocarbons are liquid if present in the condensed phase and immiscible with water. Oxidation of the precursor adds functional groups to the compounds. These functional groups lower the vapor pressure and increase viscosity (Rothfuss and Petters, 2017), density (Kuwata et al., 2012), and miscibility (Petters et al., 2016). Model calculations and experimental data suggest that adding a few hydroxyl and/or carboxylic acid groups is enough to remove miscibility limitations (Bertram et al., 2011;Petters et al., 2016) for pure organic compounds at water activity corresponding to supersaturated conditions, consistent with the results from our experiments.

~~Compounds that induce LLPS have limited miscibility with water. The net result is that LLPS can affect CCN activity in the same manner as sparingly soluble compounds (Petters et al., 2006; Petters et al., 2016). In essence, the presence of undissolved organics can be considered as a special case of LLPS (i.e., the undissolved organics form the 2nd phase). Model calculations and experimental data suggest that (Bertram et al., 2011; Petters et al., 2016). an O:C ratio of 0.5, corresponding to the oxidation level of the α-pinene SOA in this study, is sufficient to remove miscibility limitations for compounds that are composed of hydroxyl and/or acid groups (Bertram et al., 2011; Petters et al., 2016). Further discussion of LLPS on droplet activation is included in Supplementary Information.~~

The above analysis is based on *κ*-Köhler theory, in which the hygroscopic parameter *κ* is derived assuming the surface tension of water for activating droplets. Surface active compounds may reduce the surface tension, potentially altering the mechanism by which CCN activation proceeds. However, surface active compounds preferentially concentrate on the droplet surface, leading to their depletion in the droplet bulk. As a result, a reduced Raoult’s effect increases equivalent water vapor pressure, compensating the reduced water vapor pressure due to lower surface tension. While surfactants may strongly influence the shape of Köhler curve and therefore droplet growth kinetics (Ruehl et al., 2016), their impact on the effective hygroscopicity parameter is likely minor for most mixtures (Sorjamaa et al., 2004;Prisle et al., 2010;Forestieri et al., 2018;Nakao, 2017;Topping, 2010), even for very strong surfactants (Petters and Petters, 2016). Here, the main question is whether it is plausible that the interfacial mechanism can exactly compensate the predicted solubility effects reported in Fig. 2, such that the net result would be the constant κ_{org} as a function of x_{AS} reported in Fig. 1. Such hypothetical compensation cannot be replicated using theory that includes surface/bulk partitioning (see Supplementary Information). However, we note that the interplay of solubility, LLPS, and surface tension during activation remains poorly understood. Several new mechanisms have been proposed (Ruehl et al., 2016;Noziere et al., 2014;Ovadnevaite et al., 2017) although limited data are available to test these to date. A discussion of these new mechanisms is given in Supplementary Information. Until evidence is presented to the contrary, we expect that exact compensation between solubility limitations and an interfacial mechanism resulting in constant κ_{org} vs. x_{AS} is unlikely.

3.4 Potential causes for the lack of solubility limitation on the droplet activation of SOA particles

As shown by the simulations above and earlier studies (e.g., Riipinen et al., 2015), water solubility can substantially influence the CCN activation for sparingly soluble compounds with $10^{-4} < C < 0.05$. The amount of sparingly soluble species dissolved at the point of activation and therefore the effective hygroscopicity is sensitive to the water solubility, inorganic volume fraction, and particles size (Bilde and Svenningsson, 2004). Because the solubility of some major monoterpene SOA products (e.g., Pinonic acid has a solubility of 5.5×10^{-3}, Kuwata et al., 2013) falls within this range, it is surprising that κ_{org} is independent of x_{AS} and droplet activation is not limited by organic water solubility for SOA particles with x_{AS} as low as 3%. Why might this be the case?

First, SOA is a mixture of hundreds of organic compounds, some of which are sufficiently water soluble. Similar to ammonium sulfate, water uptake by these water-soluble organics increases the amount of water in the growing droplet that is available for solvation of organics with low water solubility. Such an effect is evident from the simulated κ_{org} for particles consisting of organics with a distribution of solubilities (Supplementary Information, Fig. S7). It is also worth noting that based on the O:C value of 0.33, the solubility of β-caryophyllene SOA is estimated as 7.5×10^{-4} (Kuwata et al. 2013). The measured variation of κ_{org} with x_{AS} for β-caryophyllene SOA is broadly consistent with the simulated trend for mixtures with a distribution of water solubilities shown in Fig. S7. Second, the lack of solubility limitation may be partially due to the non-ideality of the mixtures in the particle organic phase. For example, in a mixture of non-interacting solids, because the chemical potential of undissolved components is the same as pure compounds, the components behave independently of one another (i.e., solubility not affected by the presence of other solids, and the dissolution behavior of each species is the same as their behavior as pure components.). This is in essence the 2nd case described in Riipinen et al. (2015) (i.e., $\gamma_i Y_{i,wet}=1$). As secondary organic aerosols consist of a large number of compounds, the mass of each compound may be sufficiently small to completely dissolve at the point of activation. Third, bulk solubility values such as that quoted for pinonic acid are referenced against a pure crystalline reference state. These values are likely not applicable for the complex multicomponent SOA mixtures where compounds are present in an amorphous ~~organic~~ phase state (Shiraiwa et al., 2017). We note that potential miscibility limitations due to LLPS could still apply to an amorphous phase state. The amorphous phase state may either be the thermodynamic stable state (Marcolli et al., 2004), or a metastable state that formed because the nucleation step required for crystallization did not occur, even though the particle is dry (Mikhailov et al., 2009). Upon humidification of the amorphous particle in a metastable state, sparingly soluble compounds can freely partition into the liquid phase, and water uptake is continuous without the first order phase transition (e.g., Kuwata et al., 2013). Thus, the effect of sudden dissolution of a crystalline state at the saturated solution, which is underlying the solubility theory used to construct Fig. 2 does not apply.

3.5 Causes for the increasing effective organic hygroscopicity with oxidation level

Because isoprene and monoterpenes represent major biogenic SOA precursors and toluene is among the major precursors of anthropogenic SOA, the lack of solubility limitation on CCN activation shown above suggests that the increase of SOA κ_{org} with increasing O:C observed in both laboratory and field studies is unlikely due to an increase of polarity and solubility for the more oxidized organic compounds. As SOA formed in our chamber experiments have O:C closely resembling fresh, unaged SOA reported in the field measurements, and are already fully dissolved at the point of activation, we expect the CCN activation is not limited by solubility for more oxidized SOA with higher O:C ratio (i.e., more polar organic molecules). The O:C values for SOA examined in this study is listed in Table S1 of Supplementary Information. In the absence of solubility limitation, κ_{org} is essentially the same as $\kappa_{\mathrm{org,intr}}$, and is controlled mainly by molar volume (Eq. 2). This has been shown by earlier studies for pure organic compounds with sufficient solubility (Petters et al., 2009;Petters et al., 2016;Kuwata et al., 2013). As shown by Kuwata et al. (2013), the variation of organic density with O:C is relatively weak and can't explain the variation in κ_{org}. For example, the density of the SOA examined in this study varied by approximately 30% from 1.12 to 1.49 g cm^{-3}, whereas the variation of κ_{org} is more than a factor of 2, from 0.07 to 0.16. Given the relatively narrow range of SOA density, the increasing κ_{org} with O:C suggests a negative correlation between the molecular weight and O:C for secondary organic species. Such negative correlation is likely due to the following two reasons. First, secondary organic species formed from smaller precursor VOCs tend to have a lower molecular weight, and they need to be more oxidized (i.e., higher O:C) such that their volatilities are sufficiently reduced for effectively partitioning into particle phase. The lower carbon number for SOA species formed from smaller VOCs also contributes to an increased O:C ratio. This trend is evident from Fig. 3, which shows both O:C and κ_{org} are negatively correlated with carbon number of precursors for SOA examined in this study. This trend is also consistent with the negative correlation between SOA hygroscopic growth factor and the precursor molecular weight observed in a previous study (Varutbangkul et al., 2006).

Second, there are several processes, including functionalization, fragmentation, and oligomerization, during the aging of SOA, Lambe et al. (2011) studied κ_{org} of SOA generated in laboratory experiments from 14 atmospherically representative biogenic and anthropogenic VOC. They found that for SOA formed from the same VOC, increased OH exposure leads to SOA with higher κ_{org} and O:C. Such increase of κ_{org} with O:C for SOA generated from the same VOC may be partially due to fragmentation, which leads to molecules with increased O:C and lower molecular weight, therefore higher κ_{org} value (Eq. 2). This process likely contributes to the increasing κ_{org} with O:C observed for ambient aerosols as well. Insights on chemical mechanism during oxidation can be obtained by examining the Van Krevelen diagram (Heald et al., 2010), which shows the variation of H:C as a function of O:C. Lambe et al. (2011) showed that as OH exposure increases, the variation of H:C vs. O:C largely follows a line with a slope close to -0.5 for SOA formed from α-pinene, β-pinene, toluene, m-xylene, and mesitylene in an oxidation flow reactor. For SOA formed from VOC of larger molecular weight such as n-decane, n-heptadecane, and diesel fuel, the slope of (ΔH:C)/(ΔO:C) is about -0.5 when O:C ratio is above ~0.5, whereas the slope is steeper for O:C below 0.5. Ng et al. (2011) also found the variation of H:C vs. O:C follows a (ΔH:C)/(ΔO:C) slope of -0.5 for ambient secondary organic aerosols measured at all sites examined in that study. A (ΔH:C)/(ΔO:C) slope of -0.5 is consistent with the addition of a carboxylic acid group to the site of a C-C bond cleavage (Kroll et al., 2009). The net effect would be to replace a $-CH_2-$ group with a $-COOH$ group, resulting a slope of -0.5 for (ΔH:C)/(ΔO:C). As organics become more oxidized during gas phase oxidation of VOC, the dominant reaction transitions from functionalization to fragmentation (Lambe et al., 2012;Zhao et al., 2015). Other studies also suggest that at O:C value of 0.4, about 80% gas phase oxidation leads to fragmentation (Donahue et al., 2012;Jimenez et al., 2009). A fraction of the fragmented molecules, which have reduced molecular weight and higher O:C can contribute to SOA by partitioning. We note auto-oxidation can also produce highly oxidized organics that contribute substantially to SOA (Ehn et al., 2014). For heterogeneous oxidation, fragmentation completely dominates once the organics reach O:C value of 0.4, and the increase in O:C ratio upon further oxidation is due to the loss of carbon rather than the addition of oxygen (Kroll et al., 2009). As an example, the fragmentation during heterogeneous oxidation of azelaic acid leads to lower molecular weight and high κ_{org} value, albeit for hygroscopic growth under sub-saturated conditions (Cappa et al., 2011). In addition to functionalization and fragmentation discussed above, oligomerization also occurs during the formation and aging of the SOA. Laboratory-generated and ambient SOA particles may consist of substantial amount of oligomers that significantly impact SOA volatility (Kalberer et al., 2004). Several studies suggest that the formation of oligomers may occur on fast time scales, ranging from less than 1 min to ~ 30 min (e.g., Zaveri et al., 2018;Kolesar et al., 2015).

Further evidence for the fragmentation of organics during oxidation may derive from the hygroscopicity of highly oxidized SOA formed from precursors with large molecular weight. For example, highly oxidized SOA formed from n-heptadecane ($C_{17}H_{36}$) reaches a κ_{org} value above 0.2 at O:C value of 1.0 (Lambe et al., 2011). Based on the organic density estimated from the O:C value of 1.0 and Eq. 2, a κ_{org} value of 0.2 indicates a molecular weight between 130 and 160 g mol^{-1}, corresponding to molecules with 4 to 6 carbon atoms. The above estimate assumes organics are completely dissolved ~~at the point of activation~~ (i.e., $\kappa_{\mathrm{org}}=\kappa_{\mathrm{org,\ intr}}$) and that non-ideal solution effects are negligible at the point of activation. If the organics are only partially dissolved, the molecular weight would have to be even lower. As the precursor molecules have 17 carbon atoms, this indicates substantial fragmentation during the formation and oxidation of SOA, which leads to increased κ_{org}.

3.6 A model for predicting the dependence of effective organic hygroscopicity on oxidation level

Whereas the variation of precursor molecule size and fragmentation during oxidation described above explain the general trend of increasing κ_{org} with the oxidation level, laboratory SOA generated from a wide range of precursors with different vapor pressures, molecular weights and structures, exhibit nearly the same relationship between κ_{org} and O:C (Lambe et al., 2011). During the recent GoAmazon 2014/5 field campaign, κ_{org} of various SOA components was derived and the variation of κ_{org} with O:C also follows a similar relationship to that observed in laboratory studies (Thalman et al., 2017). While such a "universal" relationship allows efficient parameterization of κ_{org} based on O:C, it also raises a question why such a "universal" relationship is applicable to SOA generated from a range of precursors and under different conditions. As we show next, this "universal" relationship to a large degree derives from the interplay among molecular weight, oxidation level, and volatility in the absence of solubility limitation on droplet activation. In essence, to have sufficiently low volatility and contribute substantially to SOA, smaller organic molecules, which have higher κ_{org} values due to their lower molecular weight based on Eq. 2, need to be more oxidized (i.e., higher O:C). Taking advantage of the finding that droplet activation of representative SOA is not limited by water solubility, we construct a simple model of SOA hygroscopicity parameter based on molecular weight, oxidation level, and volatility. This simple model can reproduce the relationship between κ_{org} and O:C observed in the laboratory and field studies.

The volatility of aerosol organics can be estimated using a simple three-parameter group contribution expression (Donahue et al., 2011):

$$\log_{10} C^* = -0.475 \times (n_C - 25) - 1.7 \times n_O$$

(3)

where C^* (μg/m^3) is the volatility at 293.15 K, n_{C} and n_{O} are the number of carbon ~~number~~ and oxygen ~~number~~ atoms of organic molecules, respectively. Equation 3 indicates that adding a carbon reduces the volatility by about half a decade, while adding an oxygen atom on average reduces the volatility by approximately 1.7 decades. From Eq. 3, we can derive n_{O} as a function of n_{C} and $\log_{10}C^*$:

$$n_O = -\frac{0.475}{1.7} \times (n_C - 25) - \frac{1}{1.7}\log_{10} C^* \tag{4}$$

The hydrogen number can then be estimated using the approximation (Heald et al., 2010;Donahue et al., 2011):

$$n_H / n_C \simeq 2 - n_O / n_C \tag{5}$$

Once n_C, n_O, and n_H are available, molecular weight and the organic density can be derived from H:C and O:C ratios (Kuwata et al., 2012). The approximation of Eq. 5 has negligible impact on the molecular weight given the low atomic mass of hydrogen.

As the CCN activation of most SOA is not limited by its water solubility, κ_{org} is the same as $\kappa_{\mathrm{org,\ intr}}$, which can be derived from organic density and molecular weight using Eq. 2, assuming a van't Hoff factor of 1. Therefore, κ_{org} and O:C can be derived from n_C and $\log_{10}C^*$ by combining Eq. 2-5. As an example, Fig. 4 shows n_O, n_H, molecular weight, and κ_{org} as functions of carbon number for organic species with volatility C^* of 0.1 μg/m^3 (i.e., $\log_{10}C^*=-1$). For organic species with the same volatility, n_O decreases with increasing n_C, indicating that for organics with the same volatility, those with higher carbon number tend to be less oxidized. Despite a decreasing n_O, molecular weight increases with increasing n_C, leading to a lower hygroscopicity parameter via Eq. 2.

Obviously ambient organic aerosols exhibit a range of volatilities~~y~~. Previous studies suggest that the mean $\log_{10}C^*$ of ambient organics largely falls within the range of -5 to -1 (e.g., Saha et al., 2017;Stark et al., 2017). The value of κ_{org} derived from Eq. 2-5 is plotted against O:C for organics with $\log_{10}C^*$ value ranging from -5 to -1 in Fig. 5. For organics with the same volatility, κ_{org} increases nearly linearly with O:C ratio. Despite the four orders of magnitude difference in C^*, the derived variation of κ_{org} with O:C falls within a relatively narrow band. Figure 5 also shows the linear relationship between κ_{org} with O:C derived by Lambe et al. (2011) for laboratory generated SOA with a wide range of O:C values, SOA hygroscopicity parameter derived from this study, and hygroscopicity parameter of SOA factors derived from the measurements during the recent GoAmazon 2014/5 campaign (Thalman et al., 2017). For β-caryophyllene SOA, κ_{org} shown in Fig. 5 is the average value when x_{AS} is larger than 15% (i.e., when droplet activation is not limited by the solubility of β-caryophyllene SOA). The uncertainty range of the relationship derived by Lambe et al. (2011) is shown as the shaded area in Fig. 5. The κ_{org} values derived from both the laboratory studies and field observation largely fall within the range of κ_{org} derived from Eq. 2-5 for O:C from 0 to 1.5, indicating the simple model successfully captures the major variation of κ_{org} with O:C for SOA at droplet activation (i.e., under supersaturated conditions).

The above derivation of the relationship assumes that molecules contain only hydroxyl and carbonyl groups (Donahue et al., 2011). While the volatility of molecules with other functional groups is less accurately represented, many typical functional groups in ambient aerosol organics are reasonably approximated as carbonyls, alcohols, or some combination of the two (Daumit et al., 2013). For example, an acid group decreases saturation vapor pressure by 3.58 decades, similar to 3.4 (i.e., 1.7×2) indicated by Eq. 3. While not all functional groups (e.g., Acyclic ethers) are well represented by the above treatment (Daumit et al., 2013), we expect the general trend that n_O decreases with increasing n_C for organic compounds with the same volatility is robust. As the modeled relationship between κ_{org} and O:C falls within a relatively narrow area for organics with mean $\log_{10}C^*$ ranging from -5 to -1, the uncertainties associated with the Eq. 3 is unlikely to substantially change the modelled relationships. Similar expressions of $\log_{10}C^*$ as a function of carbon and oxygen numbers were also proposed in earlier studies (Daumit et al., 2013;Pankow and Asher, 2008;Nakao, 2017;Li et al., 2016), and they do not lead to substantial differences in the results presented below. The good agreement between the modeled relationships and those derived from laboratory and field measurements suggests that the increasing SOA hygroscopicity with O:C to a large degree derives from the relationship among molecular weight, O:C, and volatility that controls gas-particle partitioning and formation of SOA.

While the results indicate that droplet activation and κ_{org} are not limited by water solubility for most SOA, we note primary organic aerosols are often hydrophobic, and droplet activation of these particles is expected to be strongly limited by the very low solubility of primary organic species. Lambe et al. (2011) showed that the relationship between κ_{org} and O:C for oxidized POA differs from that of SOA, suggesting that at the same O:C, oxidized POA have a lower κ_{org} value than SOA due to the limitation of solubility.

4. Conclusion

Organic aerosols were generated by condensation of secondary organic species onto 50 nm ammonium sulfate seeds in a steady state environmental chamber. For SOA generated from α-pinene, Δ-3 carene, isoprene, and toluene, the effective hygroscopicity parameter of organic species remains largely constant for particles with different sulfate volume fraction, suggesting that for most SOA, the droplet activation is not limited by organic water solubility, and κ_{org} at droplet activation is controlled mainly by the molecular weight of the organic species. We note there can be exceptions to this finding. Whereas on the global scale, SOA is dominated by those formed from isoprene, monoterpene, and small aromatic hydrocarbons such as toluene, SOA produced from large alkanes and aromatics are potentially important in the urban atmosphere (Gentner et al. 2017), and their droplet activation may be limited by organic water solubility, especially when the volume fraction of inorganics in the particles is low. The absence of limitation by water solubility ~~This~~ indicates that the increase of organic hygroscopicity with the organic oxidation level cannot be attributed to higher water solubility of more oxidized organic compounds. Instead, the increase of the organic hygroscopicity with oxidation level is to a large degree due to that (a) due to gas-particle partitioning, SOA formed from smaller parent VOC molecules tend to have lower molecular weight and are more oxidized and (b) during oxidation of SOA, fragmentation reactions produce organic molecules with lower molecular weight and therefore higher hygroscopicity. Taking advantage of the finding that droplet activation of SOA is not limited by water solubility, we developed a simple model of SOA hygroscopicity based on molecular weight, oxidation level, and volatility. This model is shown to reproduce the variation of κ_{org} with O:C observed from previous laboratory and field studies. These results provide a mechanistic understanding of the variation of organic hygroscopicity, which is expected to help improve the quantification of aerosol impact on clouds and climate.

Acknowledgements

The research was conducted with funding from the Atmospheric System Research (ASR) program (Office of Biological and Environmental Research of US Department of Energy) under contract DE-AC02-98CH10886 and DE-AC05-76RL01830. MDP acknowledges additional support from Office of Biological and Environmental Research of US Department of Energy

DE-SC 0012043. We acknowledge additional support by the Atmospheric Radiation Measurement (ARM) Climate Research Facility and Environmental Molecular Sciences Laboratory (EMSL), user facilities of the United States Department of Energy, Office of Science, sponsored by the Office of Biological and Environmental Research.

Table 1. The molecular formula, molecular weight, density, and intrinsic organic hygroscopicity derived using Eq. 2 for major monoterpene SOA products. The density was calculated from O:C and O:H values (Kuwata et al., 2012).

Major monoterpene SOA Products	Molecular formula	MW (g mole^{-1})	Density (g cm^{-3})	$\kappa_{org,\ intr}$
Pinonaldehyde	$C_{10}H_{16}O_2$	168	1.06	0.11
Pinic acid	$C_9H_{14}O_4$	186	1.24	0.12
Pinonic acid	$C_{10}H_{16}O_3$	184	1.13	0.11
Norpinonic acid	$C_9H_{14}O_3$	170	1.17	0.12
3-Oxo-pina Ketone	$C_7H_8O_2$	124	1.27	0.18
Limonic acid	$C_9H_{14}O_4$	186	1.24	0.12
Limonaldehyde	$C_9H_{14}O_2$	154	1.09	0.13
7-Hydroxylimonic acid	$C_{10}H_{16}O_4$	180	1.20	0.12

Figures:

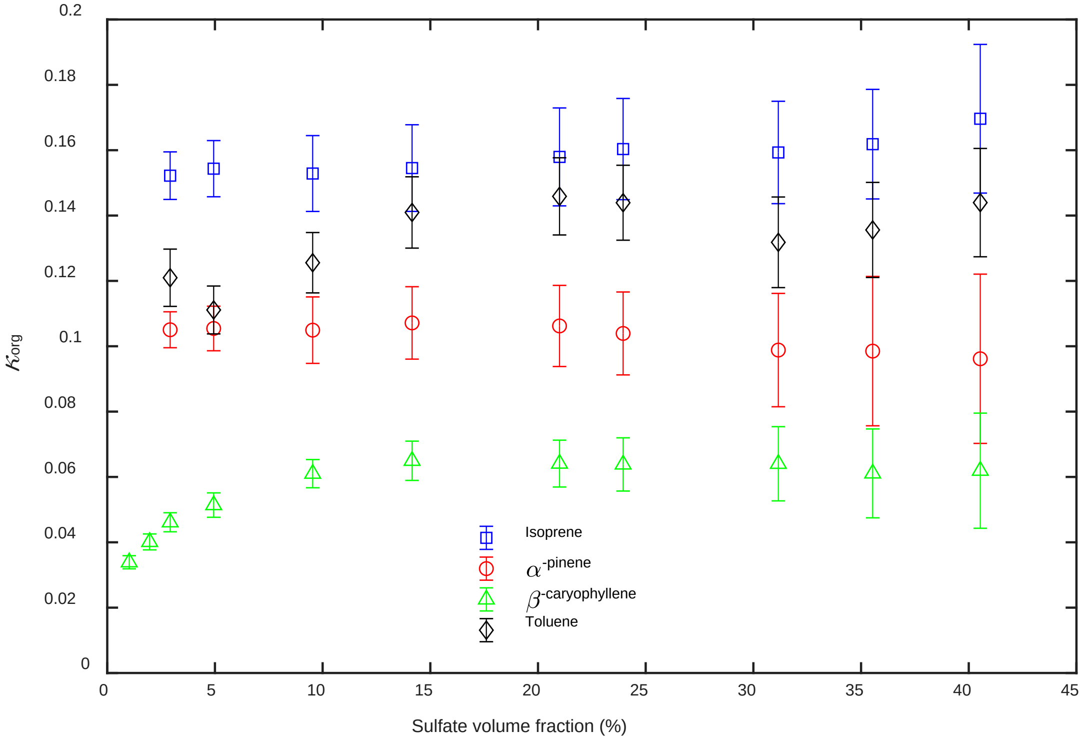

Figure 1. Effective organic hygroscopicity κ_{org} as a function of particle sulfate volume fraction for secondary organic aerosols formed from isoprene (68 g mol^{-1}), α-pinene (136 g mol^{-1}), β-caryophyllene (204 g mol^{-1}), and toluene (92 g mol^{-1}). The error bar represents the uncertainty (1-σ) of the effective organic hygroscopicity derived from size-resolved CCN measurements.

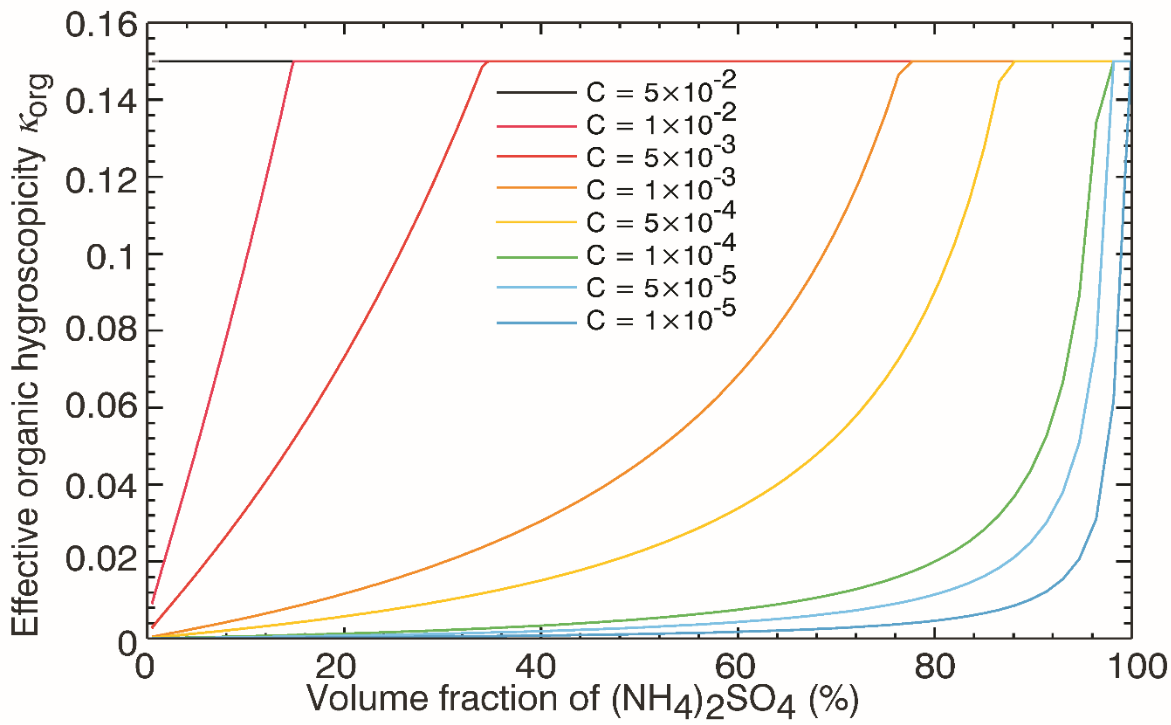

Figure 2. Simulated effective organic hygroscopicity for particles grown from 50 nm dry ammonium sulfate seeds by condensation of secondary organic species with $\kappa_{org,intr}$ = 0.15. The effective organic hygroscopicity is shown as a function of dry sulfate volume fraction for organic solubility *C* ranging from 1×10^{-5} to 5×10^{-2}.

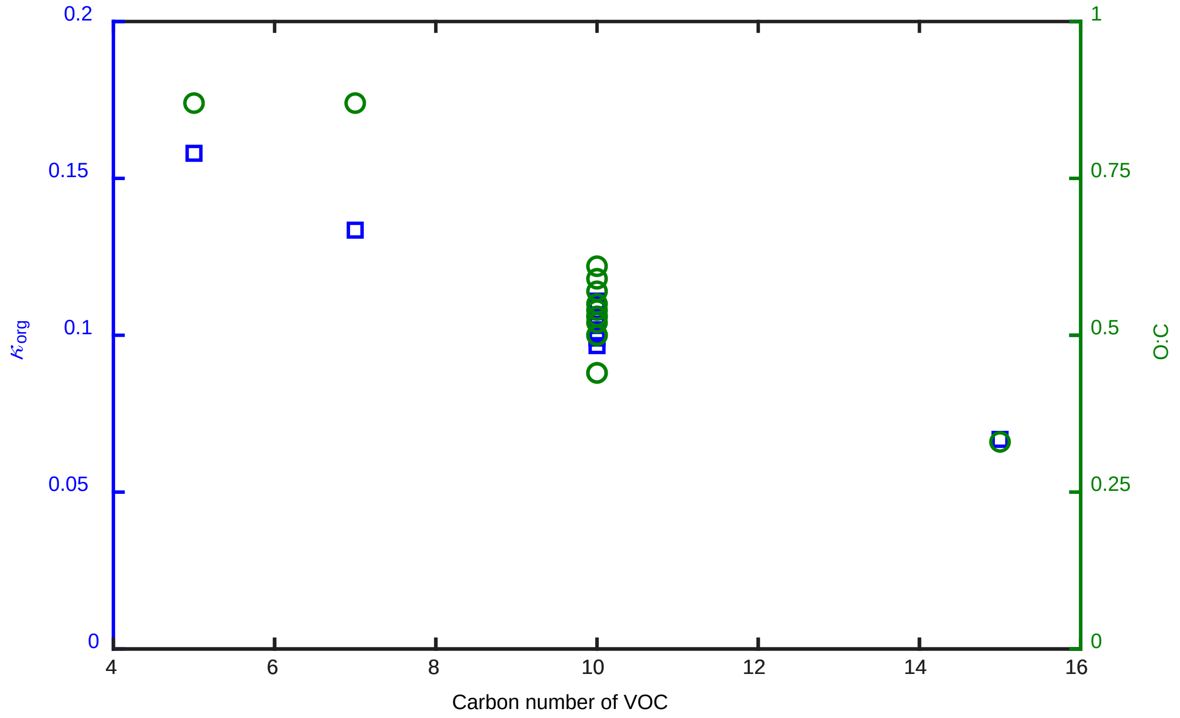

Figure 3. κ_{org} (blue square) and O:C (green circle) as a function of precursor VOC carbon number for SOA formed from isoprene, monoterpene, β-caryophyllene, and toluene in this study. For β-caryophyllene SOA, κ_{org} is the average value when x_{AS} is larger than 15% (i.e., when droplet activation is not limited by the solubility of β-caryophyllene SOA).

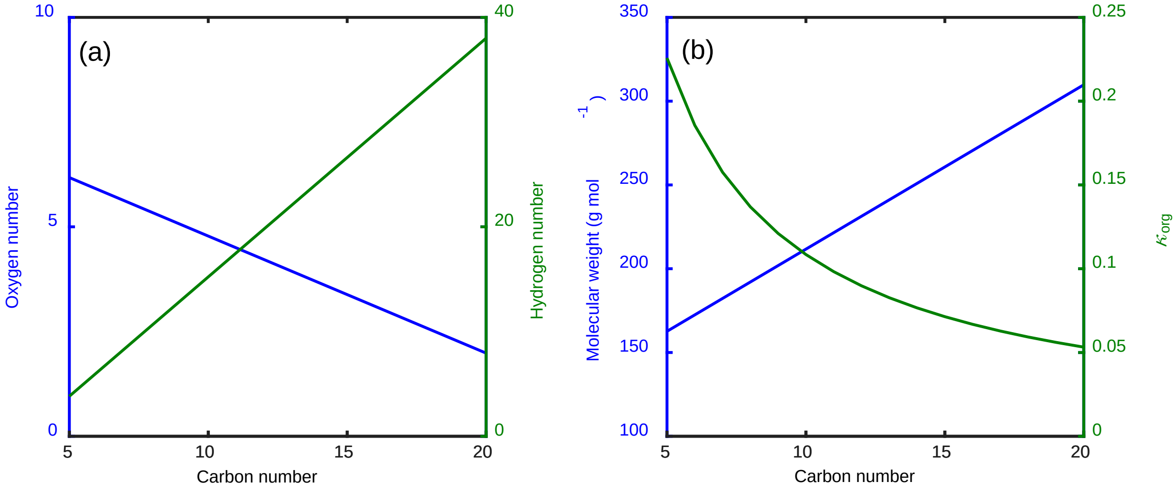

Figure 4. Oxygen and hydrogen numbers (a) and molecular weight and κ_{org} (b) as functions of carbon number for secondary organic species~~s~~ with volatility C^* of 0.1 μg/m^3 (i.e., $\log_{10}C^*$=-1)

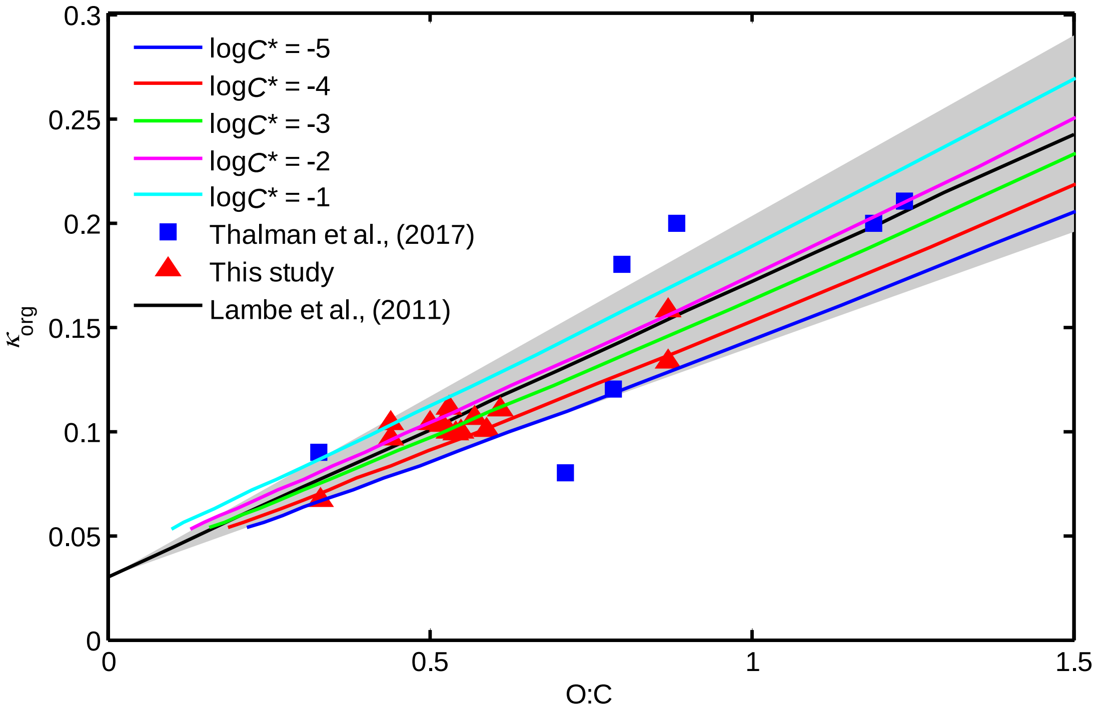

Figure 5. Predicted variation of κ_{org} as a function of O:C for organics with mean $\log_{10}C^*$ ranging from -1 to -5. Also shown are κ_{org} of SOA Positive Matrix Factorization (PMF) factors derived from measurements during GoAmazon 2014/5 (Thalman et al., 2017), κ_{org} for SOA formed from isoprene, monoterpene, β-caryophyllene, and toluene in this study, and the relationship between κ_{org} and O:C for SOA derived from a laboratory study (Lambe et al., 2011). The shaded area represents the uncertainty in the derived relationship (Lambe et al., 2011).

References:

Albrecht, B. A.: Aerosols, cloud microphysics, and fractional cloudiness, Science, 245, 1227-1230, 1989.

Alfarra, M. R., Good, N., Wyche, K. P., Hamilton, J. E., Monks, P. S., Lewis, A. C., and McFiggans, G.: Water uptake is independent of the inferred composition of secondary aerosols derived from multiple biogenic VOCs, Atmos. Chem. Phys., 13, 11769-11789, 10.5194/acp-13-11769-2013, 2013.

Asa-Awuku, A., Engelhart, G. J., Lee, B. H., Pandis, S. N., and Nenes, A.: Relating CCN activity, volatility, and droplet growth kinetics of beta-caryophyllene secondary organic aerosol, Atmos. Chem. Phys., 9, 795-812, 2009.

Bertram, A. K., Martin, S. T., Hanna, S. J., Smith, M. L., Bodsworth, A., Chen, Q., Kuwata, M., Liu, A., You, Y., and Zorn, S. R.: Predicting the relative humidities of liquid-liquid phase separation, efflorescence, and deliquescence of mixed particles of ammonium sulfate, organic material, and water using the organic-to-sulfate mass ratio of the particle and the oxygen-to-carbon elemental ratio of the organic component, Atmos. Chem. Phys., 11, 10995-11006, 10.5194/acp-11-10995-2011, 2011.

Bilde, M., and Svenningsson, B.: CCN activation of slightly soluble organics: the importance of small amounts of inorganic salt and particle phase, Tellus B, 56, 128-134, 10.1111/j.1600-0889.2004.00090.x, 2004.

Cappa, C. D., Che, D. L., Kessler, S. H., Kroll, J. H., and Wilson, K. R.: Variations in organic aerosol optical and hygroscopic properties upon heterogeneous OH oxidation, J. Geophys. Res., 116, 10.1029/2011jd015918, 2011.

Daumit, K. E., Kessler, S. H., and Kroll, J. H.: Average chemical properties and potential formation pathways of highly oxidized organic aerosol, Faraday Discuss., 165, 181-202, 10.1039/c3fd00045a, 2013.

Donahue, N. M., Epstein, S. A., Pandis, S. N., and Robinson, A. L.: A two-dimensional volatility basis set: 1. organic-aerosol mixing thermodynamics, Atmos. Chem. Phys., 11, 3303-3318, 10.5194/acp-11-3303-2011, 2011.

Donahue, N. M., Henry, K. M., Mentel, T. F., Kiendler-Scharr, A., Spindler, C., Bohn, B., Brauers, T., Dorn, H. P., Fuchs, H., Tillmann, R., Wahner, A., Saathoff, H., Naumann, K. H., Mohler, O., Leisner, T., Muller, L., Reinnig, M. C., Hoffmann, T., Salo, K., Hallquist, M., Frosch, M., Bilde, M., Tritscher, T., Barmet, P., Praplan, A. P., DeCarlo, P. F., Dommen, J., Prevot, A. S. H., and Baltensperger, U.: Aging of biogenic secondary organic aerosol via gas-phase OH radical reactions, Proc. Natl. Acad. Sci. USA, 109, 13503-13508, 10.1073/pnas.1115186109, 2012.

Ehn, M., Thornton, J. A., Kleist, E., Sipila, M., Junninen, H., Pullinen, I., Springer, M., Rubach, F., Tillmann, R., Lee, B., Lopez-Hilfiker, F., Andres, S., Acir, I. H., Rissanen, M., Jokinen, T., Schobesberger, S., Kangasluoma, J., Kontkanen, J., Nieminen, T., Kurten, T., Nielsen, L. B., Jorgensen, S., Kjaergaard, H. G., Canagaratna, M., Dal Maso, M., Berndt, T., Petaja, T., Wahner, A., Kerminen, V. M., Kulmala, M., Worsnop, D. R., Wildt, J., and Mentel, T. F.: A large source of low-volatility secondary organic aerosol, Nature, 506, 476-+, 10.1038/nature13032, 2014.

Ervens, B., Feingold, G., and Kreidenweis, S. M.: Influence of water-soluble organic carbon on cloud drop number concentration, J. Geophys. Res., 110, 10.1029/2004jd005634, 2005.

Forestieri, S. D., Staudt, S. M., Kuborn, T. M., Faber, K., Ruehl, C. R., Bertram, T. H., and Cappa, C. D.: Establishing the Impact of Model Surfactants on Cloud Condensation Nuclei

Activity of Sea Spray Aerosols, Atmos. Chem. Phys. Discuss., https://doi.org/10.5194/acp-2018-5207, 2018.

Frosch, M., Bilde, M., Nenes, A., Praplan, A. P., Juranyi, Z., Dommen, J., Gysel, M., Weingartner, E., and Baltensperger, U.: CCN activity and volatility of beta-caryophyllene secondary organic aerosol, Atmos. Chem. Phys., 13, 2283-2297, 10.5194/acp-13-2283-2013, 2013.

Guenther, A. B., Jiang, X., Heald, C. L., Sakulyanontvittaya, T., Duhl, T., Emmons, L. K., and Wang, X.: The Model of Emissions of Gases and Aerosols from Nature version 2.1 (MEGAN2.1): an extended and updated framework for modeling biogenic emissions, Geosci. Model Dev., 5, 1471-1492, 10.5194/gmd-5-1471-2012, 2012.

Heald, C. L., Kroll, J. H., Jimenez, J. L., Docherty, K. S., DeCarlo, P. F., Aiken, A. C., Chen, Q., Martin, S. T., Farmer, D. K., and Artaxo, P.: A simplified description of the evolution of organic aerosol composition in the atmosphere, Geophys. Res. Lett., 37, 10.1029/2010gl042737, 2010.

Hori, M., Ohta, S., Murao, N., and Yamagata, S.: Activation capability of water soluble organic substances as CCN, J. Aerosol Sci., 34, 419-448, 2003.

IPCC: Climate Change 2013: The Physical Science Basis: Contribution of Working Group I to the Fourth Assessment Report of the Intergovernmental Panel on Climate Change, edited by: Solomon, S. e. a., Cambridge University Press, New York, 2013.

Jimenez, J. L., Canagaratna, M. R., Donahue, N. M., Prevot, A. S. H., Zhang, Q., Kroll, J. H., DeCarlo, P. F., Allan, J. D., Coe, H., Ng, N. L., Aiken, A. C., Docherty, K. S., Ulbrich, I. M., Grieshop, A. P., Robinson, A. L., Duplissy, J., Smith, J. D., Wilson, K. R., Lanz, V. A., Hueglin, C., Sun, Y. L., Tian, J., Laaksonen, A., Raatikainen, T., Rautiainen, J., Vaattovaara, P., Ehn, M., Kulmala, M., Tomlinson, J. M., Collins, D. R., Cubison, M. J., Dunlea, E. J., Huffman, J. A., Onasch, T. B., Alfarra, M. R., Williams, P. I., Bower, K., Kondo, Y., Schneider, J., Drewnick, F., Borrmann, S., Weimer, S., Demerjian, K., Salcedo, D., Cottrell, L., Griffin, R., Takami, A., Miyoshi, T., Hatakeyama, S., Shimono, A., Sun, J. Y., Zhang, Y. M., Dzepina, K., Kimmel, J. R., Sueper, D., Jayne, J. T., Herndon, S. C., Trimborn, A. M., Williams, L. R., Wood, E. C., Middlebrook, A. M., Kolb, C. E., Baltensperger, U., and Worsnop, D. R.: Evolution of Organic Aerosols in the Atmosphere, Science, 326, 1525-1529, 2009.

Kalberer, M., Paulsen, D., Sax, M., Steinbacher, M., Dommen, J., Prevot, A. S. H., Fisseha, R., Weingartner, E., Frankevich, V., Zenobi, R., and Baltensperger, U.: Identification of polymers as major components of atmospheric organic aerosols, Science, 303, 1659-1662, 10.1126/science.1092185, 2004.

King, S. M., Rosenoern, T., Shilling, J. E., Chen, Q., Wang, Z., Biskos, G., McKinney, K. A., Poschl, U., and Martin, S. T.: Cloud droplet activation of mixed organic-sulfate particles produced by the photooxidation of isoprene, Atmos. Chem. Phys., 10, 3953-3964, 2010.

Kolesar, K. R., Li, Z. Y., Wilson, K. R., and Cappa, C. D.: Heating-Induced Evaporation of Nine Different Secondary Organic Aerosol Types, Environ. Sci. Technol., 49, 12242-12252, 10.1021/acs.est.5b03038, 2015.

Kroll, J. H., Smith, J. D., Che, D. L., Kessler, S. H., Worsnop, D. R., and Wilson, K. R.: Measurement of fragmentation and functionalization pathways in the heterogeneous oxidation of oxidized organic aerosol, Phys. Chem. Chem. Phys., 11, 8005-8014, 10.1039/b905289e, 2009.

Kuwata, M., Zorn, S. R., and Martin, S. T.: Using Elemental Ratios to Predict the Density of Organic Material Composed of Carbon, Hydrogen, and Oxygen, Environ. Sci. Technol., 46, 787-794, 2012.

Kuwata, M., Shao, W., Lebouteiller, R., and Martin, S. T.: Classifying organic materials by oxygen-to-carbon elemental ratio to predict the activation regime of Cloud Condensation Nuclei (CCN), Atmos. Chem. Phys., 13, 5309-5324, 10.5194/acp-13-5309-2013, 2013.

Lambe, A. T., Onasch, T. B., Massoli, P., Croasdale, D. R., Wright, J. P., Ahern, A. T., Williams, L. R., Worsnop, D. R., Brune, W. H., and Davidovits, P.: Laboratory studies of the chemical composition and cloud condensation nuclei (CCN) activity of secondary organic aerosol (SOA) and oxidized primary organic aerosol (OPOA), Atmos. Chem. Phys., 11, 8913-8928, doi: 10.5194/acp-11-8913-2011, 2011.

Lambe, A. T., Onasch, T. B., Croasdale, D. R., Wright, J. P., Martin, A. T., Franklin, J. P., Massoli, P., Kroll, J. H., Canagaratna, M. R., Brune, W. H., Worsnop, D. R., and Davidovits, P.: Transitions from Functionalization to Fragmentation Reactions of Laboratory Secondary Organic Aerosol (SOA) Generated from the OH Oxidation of Alkane Precursors, Environ. Sci. Technol., 46, 5430-5437, 10.1021/es300274t, 2012.

Lathem, T. L., Beyersdorf, A. J., Thornhill, K. L., Winstead, E. L., Cubison, M. J., Hecobian, A., Jimenez, J. L., Weber, R. J., Anderson, B. E., and Nenes, A.: Analysis of CCN activity of Arctic aerosol and Canadian biomass burning during summer 2008, Atmos. Chem. Phys., 13, 2735-2756, 10.5194/acp-13-2735-2013, 2013.

Li, Y., Poschl, U., and Shiraiwa, M.: Molecular corridors and parameterizations of volatility in the chemical evolution of organic aerosols, Atmos. Chem. Phys., 16, 3327-3344, 10.5194/acp-16-3327-2016, 2016.

Liu, X. H., and Wang, J. A.: How important is organic aerosol hygroscopicity to aerosol indirect forcing?, Environ. Res. Lett., 5, 10.1088/1748-9326/5/4/044010, 2010.

Marcolli, C., Luo, B. P., and Peter, T.: Mixing of the organic aerosol fractions: Liquids as the thermodynamically stable phases, J. Phys. Chem. A, 108, 2216-2224, 10.1021/jp036080l, 2004.

McFiggans, G., Artaxo, P., Baltensperger, U., Coe, H., Facchini, M. C., Feingold, G., Fuzzi, S., Gysel, M., Laaksonen, A., Lohmann, U., Mentel, T. F., Murphy, D. M., O'Dowd, C. D., Snider, J. R., and Weingartner, E.: The effect of physical and chemical aerosol properties on warm cloud droplet activation, Atmos. Chem. Phys., 6, 2593-2649, 2006.

Mei, F., Setyan, A., Zhang, Q., and Wang, J.: CCN activity of organic aerosols observed downwind of urban emissions during CARES, Atmos. Chem. Phys., 13, 12155-12169, 2013.

Mikhailov, E., Vlasenko, S., Martin, S. T., Koop, T., and Poschl, U.: Amorphous and crystalline aerosol particles interacting with water vapor: conceptual framework and experimental evidence for restructuring, phase transitions and kinetic limitations, Atmos. Chem. Phys., 9, 9491-9522, 10.5194/acp-9-9491-2009, 2009.

Moore, R. H., Cerully, K., Bahreini, R., Brock, C. A., Middlebrook, A. M., and Nenes, A.: Hygroscopicity and composition of California CCN during summer 2010, J. Geophys. Res., 117, D00V12, doi: 10.1029/2011JD017352, 2012.

Nakao, S.: Why would apparent kappa linearly change with O/C? Assessing the role of volatility, solubility, and surface activity of organic aerosols, Aerosol Sci. Technol., 51, 1377-1388, 10.1080/02786826.2017.1352082, 2017.

Ng, N. L., Canagaratna, M. R., Jimenez, J. L., Chhabra, P. S., Seinfeld, J. H., and Worsnop, D. R.: Changes in organic aerosol composition with aging inferred from aerosol mass spectra, Atmos. Chem. Phys., 11, 6465-6474, 10.5194/acp-11-6465-2011, 2011.

Noziere, B., Baduel, C., and Jaffrezo, J. L.: The dynamic surface tension of atmospheric aerosol surfactants reveals new aspects of cloud activation, Nature Communications, 5, 10.1038/ncomms4335, 2014.

Ovadnevaite, J., Zuend, A., Laaksonen, A., Sanchez, K. J., Roberts, G., Ceburnis, D., Decesari, S., Rinaldi, M., Hodas, N., Facchini, M. C., Seinfeld, J. H., and Dowd, C. O.: Surface tension prevails over solute effect in organic-influenced cloud droplet activation, Nature, 546, 637-641, 10.1038/nature22806, 2017.

Pankow, J. F., and Asher, W. E.: SIMPOL.1: a simple group contribution method for predicting vapor pressures and enthalpies of vaporization of multifunctional organic compounds, Atmos. Chem. Phys., 8, 2773-2796, 2008.

Petters, M. D., Kreidenweis, S. M., Snider, J. R., Koehler, K. A., Wang, Q., Prenni, A. J., and Demott, P. J.: Cloud droplet activation of polymerized organic aerosol, Tellus B, 58, 196-205, 10.1111/j.1600-0889.2006.00181.x, 2006.

Petters, M. D., and Kreidenweis, S. M.: A single parameter representation of hygroscopic growth and cloud condensation nucleus activity, Atmos. Chem. Phys., 7, 1961-1971, 2007.

Petters, M. D., and Kreidenweis, S. M.: A single parameter representation of hygroscopic growth and cloud condensation nucleus activity - Part 2: Including solubility, Atmos. Chem. Phys., 8, 6273-6279, 2008.

Petters, M. D., Kreidenweis, S. M., Prenni, A. J., Sullivan, R. C., Carrico, C. M., Koehler, K. A., and Ziemann, P. J.: Role of molecular size in cloud droplet activation, Geophys. Res. Lett., 36, 2009.

Petters, M. D., Kreidenweis, S. M., and Ziemann, P. J.: Prediction of cloud condensation nuclei activity for organic compounds using functional group contribution methods, Geosci. Model Dev., 9, 111-124, 10.5194/gmd-9-111-2016, 2016.

Petters, S. S., and Petters, M. D.: Surfactant effect on cloud condensation nuclei for two-component internally mixed aerosols, J. Geophys. Res., 121, 1878-1895, 10.1002/2015jd024090, 2016.

Pringle, K. J., Tost, H., Pozzer, A., Poschl, U., and Lelieveld, J.: Global distribution of the effective aerosol hygroscopicity parameter for CCN activation, Atmos. Chem. Phys., 10, 5241-5255, 10.5194/acp-10-5241-2010, 2010.

Prisle, N. L., Raatikainen, T., Laaksonen, A., and Bilde, M.: Surfactants in cloud droplet activation: mixed organic-inorganic particles, Atmos. Chem. Phys., 10, 5663-5683, 10.5194/acp-10-5663-2010, 2010.

Pye, H. O. T., Chan, A. W. H., Barkley, M. P., and Seinfeld, J. H.: Global modeling of organic aerosol: the importance of reactive nitrogen (NOx and NO3), Atmos. Chem. Phys., 10, 11261-11276, 10.5194/acp-10-11261-2010, 2010.

Rickards, A. M. J., Miles, R. E. H., Davies, J. F., Marshall, F. H., and Reid, J. P.: Measurements of the Sensitivity of Aerosol Hygroscopicity and the kappa Parameter to the O/C Ratio, J. Phys. Chem. A, 117, 14120-14131, 10.1021/jp407991n, 2013.

Riipinen, I., Rastak, N., and Pandis, S. N.: Connecting the solubility and CCN activation of complex organic aerosols: a theoretical study using solubility distributions, Atmos. Chem. Phys., 15, 6305-6322, 10.5194/acp-15-6305-2015, 2015.

Rothfuss, N. E., and Petters, M. D.: Influence of Functional Groups on the Viscosity of Organic Aerosol, Environ. Sci. Technol., 51, 271-279, 10.1021/acs.est.6b04478, 2017.

Ruehl, C. R., Davies, J. F., and Wilson, K. R.: An interfacial mechanism for cloud droplet formation on organic aerosols, Science, 351, 1447-1450, 10.1126/science.aad4889, 2016.

Saha, P. K., Khlystov, A., Yahya, K., Zhang, Y., Xu, L., Ng, N. L., and Grieshop, A. P.: Quantifying the volatility of organic aerosol in the southeastern US, Atmos. Chem. Phys., 17, 501-520, 10.5194/acp-17-501-2017, 2017.

Shilling, J. E., Chen, Q., King, S. M., Rosenoern, T., Kroll, J. H., Worsnop, D. R., McKinney, K. A., and Martin, S. T.: Particle mass yield in secondary organic aerosol formed by the dark ozonolysis of alpha-pinene, Atmos. Chem. Phys., 8, 2073-2088, 10.5194/acp-8-2073-2008, 2008.

Shiraiwa, M., Li, Y., Tsimpidi, A. P., Karydis, V. A., Berkemeier, T., Pandis, S. N., Lelieveld, J., Koop, T., and Poschl, U.: Global distribution of particle phase state in atmospheric secondary organic aerosols, Nature Communications, 8, 10.1038/ncomms15002, 2017.

Shulman, M. L., Jacobson, M. C., Carlson, R. J., Synovec, R. E., and Young, T. E.: Dissolution behavior and surface tension effects of organic compounds in nucleating cloud droplets, Geophys. Res. Lett., 23, 277-280, 1996.

Sorjamaa, R., Svenningsson, B., Raatikainen, T., Henning, S., Bilde, M., and Laaksonen, A.: The role of surfactants in Kohler theory reconsidered, Atmos. Chem. Phys., 4, 2107-2117, 2004.

Stark, H., Yatavelli, R. L. N., Thompson, S. L., Kang, H., Krechmer, J. E., Kimmel, J. R., Palm, B. B., Hu, W. W., Hayes, P. L., Day, D. A., Campuzano-Jost, P., Canagaratna, M. R., Jayne, J. T., Worsnop, D. R., and Jimenez, J. L.: Impact of Thermal Decomposition on Thermal Desorption Instruments: Advantage of Thermogram Analysis for Quantifying Volatility Distributions of Organic Species, Environ. Sci. Technol., 51, 8491-8500, 10.1021/acs.est.7b00160, 2017.

Sullivan, R. C., Moore, M. J. K., Petters, M. D., Kreidenweis, S. M., Roberts, G. C., and Prather, K. A.: Effect of chemical mixing state on the hygroscopicity and cloud nucleation properties of calcium mineral dust particles, Atmos. Chem. Phys., 9, 3303-3316, 2009.

Thalman, R., de Sa, S. S., Palm, B. B., Barbosa, H. M. J., Pohlker, M. L., Alexander, M. L., Brito, J., Carbone, S., Castillo, P., Day, D. A., Kuang, C. G., Manzi, A., Ng, N. L., Sedlacek, A. J., Souza, R., Springston, S., Watson, T., Pohlker, C., Poschl, U., Andreae, M. O., Artaxo, P., Jimenez, J. L., Martin, S. T., and Wang, J.: CCN activity and organic hygroscopicity of aerosols downwind of an urban region in central Amazonia: seasonal and diel variations and impact of anthropogenic emissions, Atmos. Chem. Phys., 17, 11779-11801, 10.5194/acp-17-11779-2017, 2017.

Topping, D.: An analytical solution to calculate bulk mole fractions for any number of components in aerosol droplets after considering partitioning to a surface layer, Geosci. Model Dev., 3, 635-642, 10.5194/gmd-3-635-2010, 2010.

Twomey, S.: Influence of pollution on shortwave albedo of clouds, J. Atmos. Sci., 34, 1149-1152, 1977.

Varutbangkul, V., Brechtel, F. J., Bahreini, R., Ng, N. L., Keywood, M. D., Kroll, J. H., Flagan, R. C., Seinfeld, J. H., Lee, A., and Goldstein, A. H.: Hygroscopicity of secondary organic aerosols formed by oxidation of cycloalkenes, monoterpenes, sesquiterpenes, and related compounds, Atmos. Chem. Phys., 6, 2367-2388, 2006.

Zaveri, R. A., Shilling, J. E., Zelenyuk, A., Liu, J. M., Bell, D. M., D'Ambro, E. L., Gaston, C., Thornton, J. A., Laskin, A., Lin, P., Wilson, J., Easter, R. C., Wang, J., Bertram, A. K., Martin, S. T., Seinfeld, J. H., and Worsnop, D. R.: Growth Kinetics and Size Distribution Dynamics of Viscous Secondary Organic Aerosol, Environ. Sci. Technol., 52, 1191-1199, 10.1021/acs.est.7b04623, 2018.

Zelenyuk, A., Yang, J., Song, C., Zaveri, R. A., and Imre, D.: A New Real-Time Method for Determining Particles' Sphericity and Density: Application to Secondary Organic Aerosol Formed by Ozonolysis of alpha-Pinene, Environ. Sci. Technol., 42, 8033-8038, 10.1021/es8013562, 2008.

Zhang, Q., Jimenez, J. L., Canagaratna, M. R., Allan, J. D., Coe, H., Ulbrich, I., Alfarra, M. R., Takami, A., Middlebrook, A. M., Sun, Y. L., Dzepina, K., Dunlea, E., Docherty, K., DeCarlo, P. F., Salcedo, D., Onasch, T., Jayne, J. T., Miyoshi, T., Shimono, A., Hatakeyama, S., Takegawa, N., Kondo, Y., Schneider, J., Drewnick, F., Borrmann, S., Weimer, S., Demerjian, K., Williams, P., Bower, K., Bahreini, R., Cottrell, L., Griffin, R. J., Rautiainen, J., Sun, J. Y., Zhang, Y. M., and Worsnop, D. R.: Ubiquity and dominance of oxygenated species in organic aerosols in anthropogenically-influenced Northern Hemisphere midlatitudes, Geophys. Res. Lett., 34, L13801, doi:10.1029/2007GL029979, 2007.

Zhao, D. F., Kaminski, M., Schlag, P., Fuchs, H., Acir, I. H., Bohn, B., Haseler, R., Kiendler-Scharr, A., Rohrer, F., Tillmann, R., Wang, M. J., Wegener, R., Wildt, J., Wahner, A., and Mentel, T. F.: Secondary organic aerosol formation from hydroxyl radical oxidation and ozonolysis of monoterpenes, Atmos. Chem. Phys., 15, 991-1012, 10.5194/acp-15-991-2015, 2015.

Zhao, D. F., Buchholz, A., Kortner, B., Schlag, P., Rubach, F., Fuchs, H., Kiendler-Scharr, A., Tillmann, R., Wahner, A., Watne, A. K., Hallquist, M., Flores, J. M., Rudich, Y., Kristensen, K., Hansen, A. M. K., Glasius, M., Kourtchev, I., Kalberer, M., and Mentel, T. F.: Cloud condensation nuclei activity, droplet growth kinetics, and hygroscopicity of biogenic and anthropogenic secondary organic aerosol (SOA), Atmos. Chem. Phys., 16, 1105-1121, 10.5194/acp-16-1105-2016, 2016.

Zuend, A., and Seinfeld, J. H.: Modeling the gas-particle partitioning of secondary organic aerosol: the importance of liquid-liquid phase separation, Atmos. Chem. Phys., 12, 3857-3882, 10.5194/acp-12-3857-2012, 2012.

Supplementary Information

Cloud droplet activation of secondary organic aerosol is mainly controlled by molecular weight, not water solubility

Jian Wang, John E. Shilling, Jiumeng Liu, Alla Zelenyuk, David M. Bell, Markus Petters, Ryan Thalman, Fan Mei, Rahul A. Zaveri, and Guangjie Zheng

1. Experimental setup

1.1 Steady state chamber experiments

Experiments were conducted in Pacific Northwest National Laboratory's 10.6 m^3 environmental chamber under a wide range of conditions. Experiments were run in the continuous-flow mode, where reactants are continuously injected into the chamber and are oxidized as they flow through it. Total flow rate through the chamber for these experiments varied between 35.7 and 48.3 l min^{-1} resulting in mean residence times of 3.7 – 4.9 hours. Effloresced ammonium sulfate particles were generated by atomizing dilute solutions of ammonium sulfate and passing the aerosol through a custom designed diffusion dryer, which was 1.83 meter long with inner diameter of 10.2 cm. The sulfate particles were then size selected at 50 nm by a differential mobility analyzer (DMA, Model 3081, TSI Inc.) operating at a sheath to aerosol flow ratio of 10:3.2 before injected into the chamber. Measurements of the size-selected seed particles by a downstream SMPS confirmed their phase state and size. Water vapor was injected into the chamber by passing an air flow through a stainless steel bubbler containing 18.2 MΩ cm MilliQ water. The flow through the bubbler was continuously varied to maintain the target RH using a feedback-control loop. VOCs were introduced into the chamber using one of two methods. Isoprene and α-pinene were continuously injected into the chamber from gas cylinders at rates controlled by a mass flow controller. β-caryophyllene, Δ-3 carene, and toluene were injected into the chamber by flowing pure air at a constant rate through a bulb containing a few drops of the pure liquid and immersed in a constant temperature bath held at 5 °C. Hydrogen peroxide was added to the chamber by injecting it into a gently warmed bulb using a syringe pump and sweeping the vapor into the chamber in a flow of pure air. When desired, NO was injected into the chamber from a gas cylinder using a mass flow controller, and O_3 was generated and introduced into the chamber by passing pure air over a Jelight model 600 ozone lamp.

Chamber RH and temperature were measured with a Rotronic SC05 sensor. UV-light was provided by 104 Q-Labs UVA-340 blacklights surrounding the chamber and its intensity in the chamber was measured in real-time using a J_{NO2} radiometer and measured $J_{NO2}=0.2$ hr^{-1}. Photolysis of H_2O_2 generated OH radical for oxidation. The radiometer measurements agreed with measurements using the photostationary state method (Holmes et al., 1973). Ozone concentrations in the chamber were monitored using a Thermo Scientific model 49i ozone sensor. NO/NOx concentrations were measured using a Thermo Scientific 42i detector. Particle size distributions were measured using scanning mobility particle sizer (SMPS) consisting of a TSI 3080 long-column DMA and a TSI 3775 CPC. Aerosol chemical composition was characterized using an Aerodyne HR-ToF-AMS (DeCarlo et al., 2006). The instrument was regularly calibrated during the experiments and data were analyzed using standard methods described in the literature (Allan et al., 2004). The collection efficiency of the AMS varied between 1 and 0.5, depending on the SOA precursor, and the relative inonization efficiency of organics was 1.4. The values of O:C and H:C were calculated using the updated fragmentation tables in Canagaratna et al. (2015). for all SOA precursors except for isoprene, which used the fragmentation tables of Chen et al. (2011). VOCs were measured using an Ionicon quadrupole

PTR-MS (Lindinger et al., 1998). The PTR-MS was regularly calibrated using a certified gas cylinder containing most of the experimental gases. Δ-3 carene and β-caryophyllene concentrations were approximated using the response factor for α-pinene. The experimental conditions are listed in Table S1 (Supplementary Information).

1.2 Size-resolved CCN measurements

The size-resolved CCN activated fraction was measured using the same system and approach described in Mei et al. (2013) and is briefly described here. Aerosol particles from the steady state chamber were first dried to below 20% relative humidity (RH), neutralized by a Kr-85 aerosol neutralizer, and subsequently classified by a DMA. The classified aerosol was then simultaneously characterized by a condensation particle counter and a CCN counter (Model CCN-100, Droplet Measurement Technologies, Inc.). The sample and sheath flows of the DMA were maintained at 0.89 and 8.9 L min^{-1}, respectively. The total flow of CPC was reduced to 0.39 L min^{-1} and the sample flow of the CCN counter was maintained at 0.5 L min^{-1}.

The longitudinal temperature gradient of the CCN counter was stepped through 4.55, 4.7, 4.85, 5.0, 5.3, 5.5, 5.65, 6.0, 6.4, 6.9, 7.8, 8.5, 9.3 °C, which corresponded to supersaturations (*S*) ranging from ~0.1% to ~0.6%. The supersaturation inside the CCN counter was maintained at each value for approximately 8 minutes, during which the diameter of particles classified by the DMA was scanned between 30 nm and 315 nm twice, with each scan lasting 180 seconds . Immediately following each change of temperature gradient (i.e., supersaturation), the system waited for 90 seconds to ensure that the temperatures stabilized before the next scan of particle size commenced. The CCN counter was stepped through the above 13 *S* values approximately every 100 minutes. The aerosol size distribution was derived by inverting the particle concentration measured by the CPC using a routine described in Collins et al. (2002). The same procedure was also applied to the measured CCN concentration to obtain CCN size distribution. The ratio of the inverted CCN and aerosol size distributions provided size-resolved CCN activated fraction.

The CCN counter was calibrated at the 0.5 L min^{-1} sampling flow rate, and under the 13 temperature gradients using ammonium sulfate particles before and after the experiments during the summer of 2015 and again before and after the experiments in February of 2016. The instrument supersaturation was derived from Köhler theory using a constant van’t Hoff factor of 2.5 for ammonium sulfate. Since both sample pressure and temperature were essentially identical during measurements and calibrations, no temperature or pressure correction of the calibrated supersaturation is necessary.

We note some of the volatile SOA species may evaporate as a result of the heating inside CCN counter growth column (e.g., Asa-Awuku et al., 2009). However, CCN are quickly activated inside the growth column (i.e., within 10 seconds), and once activated, the evaporation of volatile species is likely slow. As the CCN remains un-activated near the top of the growth column, where temperature is very close to the room temperature, we expect overall effect on CCN measurements due to the evaporation is minor. Co-condensation of water soluble vapors during droplet growth lowers the supersaturation required for CCN activation (Topping et al., 2013). On the other hand, because the surface area of the wetted growth column inner wall is much larger than that of the activating particles, vast majority of the water soluble vapors is expected to be uptaken by the wetted innner wall, therefore the effect of co-condensation on measurements by the CCN counter is expected to be minimal.

~~2. Uncertainty of derived effective organic hygroscopicity~~

~~As organic particles formed by condensational growth of ammonium sulfate seeds are spherical (Zelenyuk et al., 2008b), no shape factor correction is necessary for the derivation of particle κ from the measured particles sizes. The impact of coagulation is minor under the experimental conditions. The value of κ_{org} was derived from Eq. 1 in the main text, therefore its uncertainty derives from the uncertainties of particle κ and sulfate volume fraction. As particle κ was derived from the activation spectrum (the variation of activated fraction as a function of supersaturation) of size-selected particles, the uncertainty in particle κ can be attributed to the uncertainties in particles size, supersaturation of CCN counter, and activation fractions. The uncertainty in sulfate volume fraction derives from the uncertainties in the mode diameters of ammonium sulfate seeds and grown particles size-selected for CCN measurements.~~

~~Given the steps involved in the derivation of κ_{org}, it is difficult to obtain the uncertainty of κ_{org} analytically through error propagation. Instead, the uncertainty was calculated numerically using a Monte Carlo approach described as follows. The CCN counter supersaturation, activation fraction, and the mode diameters of ammonium sulfate seeds and grown particles size-selected for CCN measurements were randomly chosen from normal distributions with respective mean values and standard deviations. These randomly chosen parameters were then used to calculate κ_{org} following the method described in the main text. The above calculation was repeated 100 times, and the uncertainty of κ_{org} was derived from the distribution of the 100 κ_{org} values. The distribution of CCN counter supersaturation was assumed as a normal distribution, and the mean and standard deviation of the distribution was derived from the repeated calibration values (e.g., Fig. 1 in the main text). The mode diameter of ammonium sulfate seeds, the mode diameter of grown particles size-selected for CCN measurements, and the activated fraction were assumed to~~

~~have normal distributions with standard deviations as 1%, 1%, and 5% of the mean values, respectively.~~

~~3.~~2. Impact of particles grown from doubly charged seeds on derived organic hygroscopicity

In addition to the singly-charged 50 nm ammonium sulfate (AS) seeds, the DMA also selects doubly-charged AS particles with a mode dimeter of 72.6 nm. Particles grown on the doubly charged seeds have a higher sulfate volume fraction compared to those of the same size but grown on singly charged seeds, therefore higher particle hygroscopicity. The derivation of particle κ and κ_{org} therefore requires the knowledge of the fraction of particles grown from doubly charged seeds. Let $n_{1,0}(D_p)$ and $n_{2,0}(D_p)$ represent the size distribution of singly and doubly charged ammonium sulfate seeds introduced into the chamber, and $n_1(D_p)$ and $n_2(D_p)$ represent particles exiting the chamber that are grown on the singly and doubly charged seeds, respectively. The fraction of sampled particles that are grown from doubly charged seeds, $f_2(D_p)$ is given by $f_2(D_p) = n_2(D_p) \big/ \left(n_1(D_p) + n_2(D_p) \right)$. Figure S2 shows an example of the seed particle size distribution measured on July 10th, 2015, $n_{1,0}$ and $n_{2,0}$ were derived by fitting the measured size distribution using lognormal modes. The result shows that the population of doubly charged seeds represented a very minor (number) fraction of the total seeds introduced into the chamber.

The fraction of particles grown from doubly charged seeds and its variation with particle diameter are influenced by several factors and are difficult to obtain based on calculations alone. In this study, we derive $f_2(D_p)$ by combining direct measurements of $f_2(D_p)$ at 100 nm and simulated spectral profile of $f_2(D_p)$. The procedure is detailed below. For grown particles that are size-selected at 100 nm, there are two populations, one with singly charged AS seed and a nominal 25 nm thick SOA coating, and others with doubly charged AS seed and a 13.7 nm thick SOA coating. These particles have essentially the same mobility diameter, but different densities, and thus different vacuum aerodynamic diameters (D_{va}) (Zelenyuk et al., 2008a). Having the same mobility diameters and spherical shape, the detection efficiency of these two particle types is identical, as is the transmission through the inlet of single particle mass spectrometer, miniSPLAT (Zelenyuk et al., 2015), used to measure their D_{va}, shape, density, and composition. Figure S3 provides, an example, D_{va} distributions of SOA-coated AS particles classified with mobility diameters of 100 nm. The first peak corresponds to particles with lower density, containing singly charged AS seeds, while the second peak is of particles grown on doubly charged AS seeds. Also shown is the fit of the data with two peaks. The value of $f_2(D_p)$ at 100 nm can be straightforwardly derived from the areas of the two peaks that reflect the relative abundance of two particle populations in the sample.

To obtain the spectral profile of $f_2(D_p)$, we first simulate the size distributions of particles grown from singly and double seeds from $n_{1,0}$ and $n_{2,0}$ using a model presented in Seinfeld et al. (2003). In this model, particle growth is treated as condensation of two empirical species, and the growth rate is expressed as:

$$I(D_p) = \frac{dD_p}{dt} = \beta_A \frac{f(Kn_A)}{D_p} + \beta_B \frac{f(Kn_B)}{D_p} \tag{S1}$$

Where β_i is related to the product of the molecular diffusivity, molecular weight, and the vapor pressure difference between the surrounding atmosphere and that above the particle surface for species i, and

$$f(Kn_i) = f\left(\frac{\lambda_i}{D_p}\right) = \frac{1}{1+\frac{\lambda_i}{D_p}} \quad \text{(S2)}$$

where λ_i is the mean free path of species i. With the four parameters β_A, β_B, λ_A, and λ_B, mean residence time of particles in the chamber (τ), and particle wall loss coefficient (α), we can derive $n_1(D_p)$ and $n_2(D_p)$ and therefore $f_2(D_p)$ from $n_{1,0}(D_p)$ and $n_{2,0}(D_p)$ using the model. The mean residence time ranged from 3.7 to 4.9 hours for the experiments. Figure S4 shows $f_2(D_p)$ as a function of D_p derived from seed particle size distributions shown in Fig. S2 using τ of 4.3 hours, and a set of representative parameters (i.e., α = 0.027 h^{-1}, β_A=1.5×10^{-6} $\mu m^2 s^{-1}$, β_B=2.5×10^{-7} $\mu m^2 s^{-1}$, λ_A = 17 nm, and λ_A = 21 nm) reported in Seinfeld et al. (2003). $f_2(D_p)$ starts with a low value (~ 2%) at 52 nm, and it increases with D_p, and reaches a plateau of 18% at ~ 100 nm.

To examine the dependence of $f_2(D_p)$ spectral profile on model parameters, we introduce a normalized $f_2(D_p)$ as:

$$\overline{f_2(D_p)} = f_2(D_p) \big/ \max\left[f_2(D_p) \right]$$

The dependences of $\overline{f_2(D_p)}$ on α, β_i, λ_i values are shown in Fig. S5. $\overline{f_2(D_p)}$ shows negligible variation for two orders of magnitude change in α, β_i, or λ_i. The profiles consistently show that $f_2(D_p)$ reaches its plateau at ~100 nm. Therefore, we combine $\overline{f_2(D_p)}$ and f_2 measured at 100 nm to derive f_2 at the size of particles sampled by the size resolved CCN system.

At a given particle size, the influence of particles grown from doubly charged seeds on derived κ_{org} is taken into consideration using the following approach. Particles grown from doubly charged seeds have higher sulfate volume fraction, and therefore low critical supersaturation. Let S_c denote the critical supersaturation for size-selected particles grown from singly-charged 50 nm seeds. Assuming particles grown from double charged particles are all activated at S_c due to their higher hygroscopicity, we derive S_c as the supersaturation at which the activated fraction reaches 50%×(1- f_2) + f_2 = 50%× (1+ f_2). The overall particle κ is then derived from particle diameter and S_c using the approached described in earlier papers (e.g., Mei et al., 2013). For the isoprene and monoterpene experiments, the average f_2 at 100 nm was 15% with a standard deviation of 5%. For the β-caryophyllene experiment, f_2 at 100 nm was measured as 5% while no data were available for the Toluene experiment. In this study, we used 15% for f_2 at 100 nm for isoprene and monoterpene experiments, and 5% for β-caryophyllene and toluene experiments. Changing f_2 at 100 nm for the isoprene and monoterpene experiments to 10% or 26% (i.e., minimum and maximum measured during these experiments) or changing f_2 at 100 nm to 2.5% or 10% for the β-caryophyllene and toluene experiments leads negligible change in the trend of κ_{org} with x_{AS} shown in Fig. 1 and Fig. S1.

~~4.~~3. Examples of Köhler curve for mixtures of sulfate and sparingly soluble organics

The Köhler curve (blue line in Fig. S6) was calculated for mixtures of ammonium sulfate and sparing soluble organics with solubility C of 0.01. The volume of sulfate inside the particles is equivalent to a 50 nm sulfate particle, same as particles formed in the steady state chamber. As the droplets grow, and fraction of dissolved organics increases, eventually reaches 100% (Fig. S5). This gradual increase of h leads to two (local) maxima of the Köhler curve (Fig. S6). The relative magnitude of the supersaturation maxima varies with the volume fraction of the sparingly soluble organics. For particles with sulfate volume fraction of 0.1 (diameter of 108 nm), the first maximum dominates and represents the critical supersaturation of 0.29%, at which point 32% of the sparingly soluble organics are dissolved. For particle with sulfate volume fraction of 0.2, the 2nd maximum becomes the highest point of the Köhler curve at 0.32%. In this case, all organics are dissolved at the point of activation, and the effective organic hygroscopicity is the same as the intrinsic organic hygroscopicity, therefore not limited by the organic water solubility.

~~5.~~4.Simulation of κ_{org} for particles consisting of organics with a distribution of solubility

The effective organic hygroscopicity κ_{org} were also simulated for particles composed of ammonium sulfate seed and model organic compounds with $\kappa_{org,\ intr}$ of 0.15 and various assumptions of the solubility distribution. The results are shown in Fig. S7. For these simulations, 61 compounds were used. All compounds have the same $\kappa_{org,\ intr} = 0.15$ and their water solubility is lognormally distributed as shown in panels (b), (d), and (f). Each bin represents a compound and the fraction of each bin in the plotted distribution corresponds to the volume fraction of the compound with the corresponding solubility in the organic phase. The mode of the solubility distribution is fixed according to the isolines selected for simulations in panels (a), (c), and (e), with the mode solubility C_m varying from 5×10^{-2} to 1×10^{-5}. The top row corresponds to a geometric standard deviation $\sigma_g = 1$ for the solubility distribution. This simulation corresponds to the single solubility simulation shown Fig. 2 of the main text. The second row corresponds to a narrower set of solubility distributions with $\sigma_g = 2$ and the bottom row to wider set of solubility distributions with $\sigma_g = 3$. The dissolution of each organic compound is assumed not affected by the presence of other organics in the particle phase for the simulations.

Figure S7 shows how changing from a single organic compound to a multicomponent mixture with distributed solubility affects the x_{AS} value where the simulated κ_{org} approaches the plateau at the intrinsic $\kappa_{\mathrm{org,\ intr}}$. The wider the distribution, the lower is the x_{AS} where the plateau is reached for selected mode solubility. This is partially due to the right tail of the solubility distribution. These compounds are more soluble than the mode solubility and therefore dissolve at lower water contents. Not unexpectedly the entire aerosol is more easily dissolved in the distributed simulations. One peculiar case is the $C = 10^{-3}$ simulation shown in Fig. S7 (e). At low x_{AS}, the addition of sulfate appears to make the aerosol less soluble, manifesting itself in a decrease in κ_{org}. At first glance this should not occur, as adding ammonium sulfate should always add additional water that aides the dissolution of the organics. One hidden feature in these simulations is that the particle size is not constant. Volume fraction is varied by starting with a 50 nm AS core and high organic fractions are achieved by very thick coatings of organic material. This implies that increasing x_{AS} corresponds to decreasing particle size in the simulations. Generally, this has only a small influence on the result. However, in cases where the solubility is just right, the increasing Kelvin effect can decrease the total particle water content and thus compensate for the increasing water content by the added sulfate. This explains the dip in the $C = 10^{-3}$ simulation in Fig. S6 (e). This behavior occurs in a very narrow range of solubility that is unlikely replicable in actual experiments. The general conclusion from these simulations is that the broader the distribution of solubility, the more the sparingly soluble range is shifted toward lower solubilities. Compounds with $C < 1\times10^{-5}$ remain effectively insoluble, except when present in predominately inorganic particle matrices.

~~6. Solubility, miscibility, liquid-liquid phase separation, and CCN activation~~

~~Solubility refers to the amount of material present in the saturated solution. For an initially dry particle, solubility and water activity of the saturated solution will control the size and RH at which pure crystalline substances spontaneously dissolve (Bilde and Svenningsson, 2004; Hori et al., 2003; Petters and Kreidenweis, 2008; Shulman et al., 1996). For particles that include sparingly soluble compounds, the dissolution occurs in the supersaturated regime and thereby exerts some control over the critical supersaturation. This gives rise to strong sensitivity of~~ ~~κ_{org}~~ ~~with increasing inorganic fraction. Miscibility is related to solubility and refers to the ability of two liquid phases to mix. Substances that form two liquid phases are immiscible. If a miscibility transition occurs in the supersaturated regime, miscibility limitations exert a similar control over critical supersaturation as solubility (Petters et al., 2006; Petters et al., 2016), i.e., the effective hygroscopicity~~ ~~κ_{org}~~ ~~observed from CCN activation is reduced at lower net water contents (smaller size or less hygroscopic material present). Distinguishing between miscibility and solubility in CCN experiments is not possible because the manifestation of the effect is identical.~~

~~In general, SOA precursors are weakly oxidized hydrocarbons. These hydrocarbons are liquid if present in the condensed phase and immiscible with water. Oxidation of the precursor adds functional groups to the compounds. These functional groups lower the vapor pressure and increase viscosity (Rothfuss and Petters, 2017), density (Kuwata et al., 2012), and miscibility (Petters et al., 2016). Model calculations and experimental data suggest that at O:C ratios of 0.5 or higher, miscibility limitations become negligible for compounds that are composed of hydroxyl and/or acid groups (Bertram et al., 2011; Petters et al., 2016).~~

~~7.~~5. Solubility, surface tension, and CCN activation

One hypothesis for the observed near constant κ_{org} is that surface tension and solubility effects conspire to produce this result. Here we use simulations to demonstrate how model predictions would change if the organic phase was strongly surface active. To do so, we combine the models of Petters and Kreidenweis (2008, 2013) that treat limited solubility and the surface tension reduction. The model equations are taken from the original publications and are summarized in Table S2. Key model parameters are listed in Table S3. Sorption isotherms for the systems studied here are not available. Therefore, model calculations were performed for a series of hypothetical sorption isotherms assuming molar volume $\alpha = 1.8 \times 10^{-4}\, m^3\, mol^{-1}$, surface excess $\Gamma_{max} = 5 \times 10^{-6}\, mol\, m^{-2}$, inverse activity coefficient $\beta = \{0.1, 10, 1000\}\, mol\, m^{-3}$, and critical micelle concentration $cmc = 0.03\, J\, m^{-2}$. The molar volume corresponds to a $\kappa_{org,intr}$ value of 0.1. A detailed literature review of sorption isotherms for several compounds is provided in Fig. 1 of Petters and Petters (2016). Figure S8 (a) illustrates the assumed isotherms for the simulations here. The three model sorption isotherms circumscribe scenarios of strong and weak surface activities. The range of water content at the point of activation is computed as in Petters and Petters (2016) and indicated on the graph. The critical micelle concentration determines the lowest possible surface tension of the solutions. The value of 0.03 J m^{-2} was selected to approximately correspond to typical values found for surfactants (see Fig. 1 of Petters and Petters, 2016). Simulations were also performed for a range of assumed solubilities spanning $C = \{\infty, 0.01, 0.001\}$. Reference calculations for the surface tension of pure water, $\sigma = 0.072\, J\, m^{-2}$, are also included. All calculations were performed starting with a 50 nm AS core particle and varying over a range of organic coating thickness corresponding to 70 – 300 nm grown particle diameter, as in the calculations shown in Fig. 2.

Figure S8 demonstrates that for a non-dissociating surfactant, the predicted κ_{org} is similar to the values predicted assuming the surface tension of pure water. This is because partitioning to the surface results in loss of bulk water, which reduces the water content relative to the reference case of no surface tension reduction. Note that this behavior is consistent with experimental CCN data for pure and internally mixed surfactants (Petters and Petters, 2016; Prisle et al., 2010). The model calculations show that treating the organic phase as surface active will not alter the solubility signature shown in Fig. 2 of the main text.

We note that the interplay of solubility, liquid-liquid phase separation, and surface tension during activation remains poorly understood. Several new mechanisms have been proposed (Noziere et al., 2014; Ovadnevaite et al., 2017; Ruehl et al., 2016), however, limited data are available to test these to date. Using measurements at Mace Head, Ovadnevaite et al. (2017) showed that for most of the time, calculated CCN concentration assuming a surface tension of water agreed well with the measured. However, during periods when organics were mixed with inorganic salt solutions in nascent ultrafine mode (i.e., particle diameter between 10 nm and 50 nm), the measured CCN concentration was significantly higher than the calculation based on measured chemical composition and the surface tension of water, but could be reproduced by assuming a much lower surface tension of ~ 50 mN m^{-1}. Ovadnevaite et al. (2017) suggested that LLPS leads to complete or partial engulfing of a hygroscopic particle core by a hydrophobic organic-rich phase. This results in substantial decrease of surface tension without a reduction of the Raoult’s effect, leading to higher CCN activity. Simulations based on this LLPS model suggest the effect of reduced surface tension on CCN activity is more pronounced for ultrafine particles, and the effect is much weaker for particles with larger diameters studied here. One prediction of the model is that particles with different organics to sulfate mass ratios (i.e.

sulfate volume fraction) exhibit similar effective hygroscopicity parameter. Such behavior is explained by that a decrease in sulfate content, and therefore the Raoult's effect, is compensated for by a prolonged surface tension lowering (to larger diameters during droplet activation) due to a larger relative amount of organics (Ovadnevaite et al., 2017). This trend is very different from the results of SOA examined in this study, which show a nearly constant κ_{org} therefore lower effective hygroscopicity parameter for particles with high organics to sulfate mass ratio.

Ruehl et al. (2016) measured droplet diameters at the point of CCN activation for particles composed of dicarboxylic acids or SOA and ammonium sulfate. They found that critical droplet diameters were 40 to 60% larger than predicted if the organic was assumed to be dissolved within the bulk droplet. The larger critical droplet diameter was attributed to surface tension depression by interfacial organic molecules, which can alter the relationship between water vapor supersaturation and droplet size (i.e., the Köhler curve). The same experiment approach was recently applied by Forestieri et al. (2018) to systems resembling those of marine aerosol. The results show that while surface tension depression by interfacial organic molecules may strongly influence the shape of Köhler curve, the net effect on critical supersaturation, and therefore effective hygroscopicity is generally minor. Therefore, until evidence is presented to the contrary, we expect that exact compensation between solubility limitations and an interfacial mechanism resulting in constant κ_{org} vs. x_{AS} for the SOA examined in this study is unlikely.

Table S1. Conditions of the steady state chamber experiments in this study. Also listed are the values of κ_{org}, O:C, and H:C for each experiment. Reactant concentrations in the inflow of the chamber air are listed. Unless otherwise noted, experiments were conducted with UV lights on and at 50% RH.

Exp. Date	Experiment condition	κ_{org}	O:C	H:C
6/21/2015	α-pinene 10 ppb, H_2O_2 5 ppm	0.10	0.55	1.8
6/22/2015	α-pinene 10 ppb, H_2O_2 0.5 ppm	0.10	0.52	1.72
6/25/2016	Δ-3 carene 10 ppb, H_2O_2 0.5 ppm	0.10	0.53	1.76
6/26/2015	Δ-3 carene 10 ppb, H_2O_2 0.25 ppm	0.10	0.54	1.75
6/27/2015	α-pinene 10 ppb, H_2O_2 1 ppm	0.10	0.5	1.74
7/1/2015	α-pinene 10 ppb, H_2O_2 1 ppm, NO 5 ppb	0.10	0.5	1.69
7/2/2015	α-pinene 10 ppb, H_2O_2 1 ppm, NO 10 ppb	0.11	0.53	1.67
7/3/2015	α-pinene 10 ppb, H_2O_2 1 ppm, NO 25 ppb	0.11	0.57	1.63
7/7/2015	α-pinene 20 ppb, H_2O_2 1 ppm, O_3 60 ppb	0.10	0.44	1.69
7/8/2015	α-pinene 20 ppb, H_2O_2 1 ppm, O_3 60 ppb, 2×residence time[a]	0.10	0.44	1.69
7/12/2015	α-pinene 10 ppb, H_2O_2 5 ppm, O_3 80 ppb, dark	0.10	0.59	1.63
7/14/2015	α-pinene 10 ppb, cyclohexane 10 ppm, O_3 80 ppb, NO 25 ppb	0.11	0.61	1.65
9/2/2015	Isoprene 15 ppb, H_2O_2 5 ppm	0.16	0.87	2.13
2/14/2016	β-caryophyllene, H_2O_2 1 ppm, <5% RH;	0.07[b]	0.33	1.72
2/22/2016	Toluene 110 ppb, H_2O_2 5 ppm, <5% RH;	0.13	0.87	1.57

[a] Mean residence time increased to 7.4 hours.

[b] Average value when sulfate volume fraction is greater than 15% (i.e., when droplet activation is not limited by the water solubility of β-caryophyllene SOA.)

Table S2. Equations used in the model for predicting effective hygroscopicity of organic surfactants with limited solubility (Petters and Kreidenweis, 2008, 2013).

Equation	**Description**
$A = \pi D^2$	Surface area of droplet
$V = \frac{\pi}{6} D^3$	Volume of entire droplet
$V_s^t = \frac{\pi}{6} D_d^3$	Volume of dry particle
$g = \frac{D}{D_d}$	Growth factor
$f_{sft} = C(g^3 - 1)\epsilon_{sft}^{-1}$	Fraction of surfactant dissolved based on bulk solubility ($f_{sft} = [0..1]$)
$V_{sft} = f_{sft}\epsilon_{sft}V_s^t$	Volume of surfactant dissolved in the droplet
$V_{sft}^b = \frac{\alpha_{sft}(g + \sqrt{g^2 + 4\varepsilon_{sft}V_s^t \beta V / \alpha_{sft}})}{2}$ $g = \frac{\varepsilon_{sft}V_s^t}{\alpha_{sft}} - \beta V - \frac{A\Gamma_{\max}}{\nu}$	Volume fraction of dissolved surfactant in the bulk based on approximation described in Raatikainen and Laaksonen (2011).
$\sigma_{s/a} = \sigma_0 - RT\Gamma_{\max} \ln\left(1 + \frac{V_{sft}^b}{\alpha_{sft}\beta V}\right)$ $\boldsymbol{\sigma_{s/a} = \sigma_{cmc}}$ if $\boldsymbol{\sigma_{s/a}}$ evaluates too low	Sorption isotherm from Szyskowski equation based on bulk dissolved surfactant
$\boldsymbol{\xi = \frac{V_{sft}^b}{V_{sft}}}$	Surface/bulk partitioning fraction
$\boldsymbol{\kappa = \epsilon_{sft}\xi f_{sft}\kappa_{sft} + (1 - \epsilon_{sft})\kappa_{core}}$	Kappa mixing rule accounting for solubility and surface partitioning. Note that for no surfactant partitioning and infinite solubility $\xi = 1$ and $f_{sft} = 1$.
$S(D) = \frac{D^3 - D_d^3}{D^3 - D_d^3(1-\kappa)} \exp\left(\frac{A\sigma_{s/a}}{TD}\right)$	The equation from which S_c is determined and κ_{org} is inferred.

Table S3. Key parameters of the model used to predict effective hygroscopicity of organic surfactants with limited solubility (Petters and Kreidenweis, 2008, 2013). Assumed quantities are marked in red.

Parameter	**Description**
$D_d\ (m)$	Dry particle diameter (assumed)
$D\ (m)$	Wet droplet diameter (derived)
$A\ (m^2)$	Wet surface area (derived)
$V\ (m^3)$	Wet particle volume (derived)
$V_s^t\ (m^3)$	Dry particle volume (derived)
$g\ (-)$	Growth factor (derived)
$\Gamma_{max}\ (mol\ m^{-2})$	Maximum surface excess (assumed)
$\beta\ (mol\ m^{-3})$	Inverse activity coefficient (assumed)
$C\ \left(\frac{m^3\ solute}{m^3\ water}\right)$	Solubility in water (assumed)
$\alpha\ (m^3\ mol^{-1})$	Molar volume of surfactant (assumed)
$\kappa_{sft}\ (-)$	κ of surfactant (assumed or derived from α)
$\kappa_{core}\ (-)$	κ of the ammonium sulfate core (assumed $\kappa_{core} = 0.6$)
$\epsilon_{sft}\ (-)$	Volume fraction of surfactant in dry particle. Calculated from core diameter (50 nm) and total particle diameter.
$\sigma_{cmc}\ (J\ m^{-2})$	Lowest allowed surface tension (assumed)

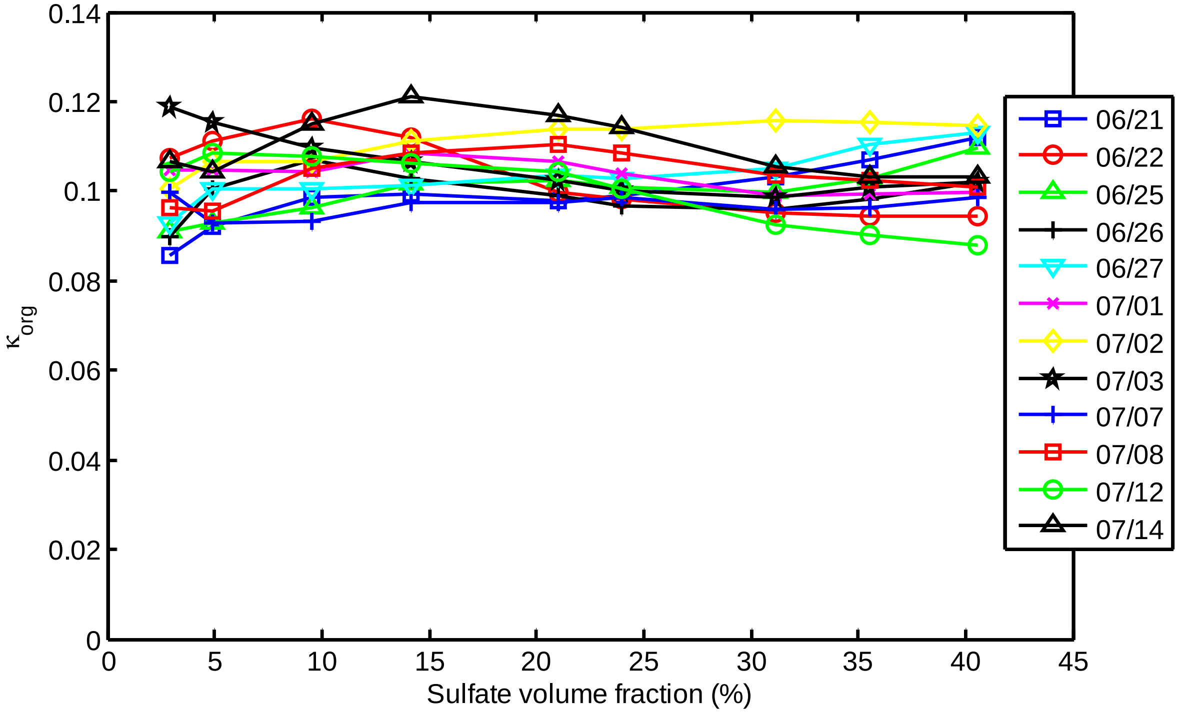

Figure S1. Effective organic hygroscopicity as a function of particle sulfate volume fraction for secondary organic aerosols formed from α-pinene and Δ-3 carene under a variety of conditions. The legend refers to the experiment date. The condition for each experiment is detailed in Table S1.

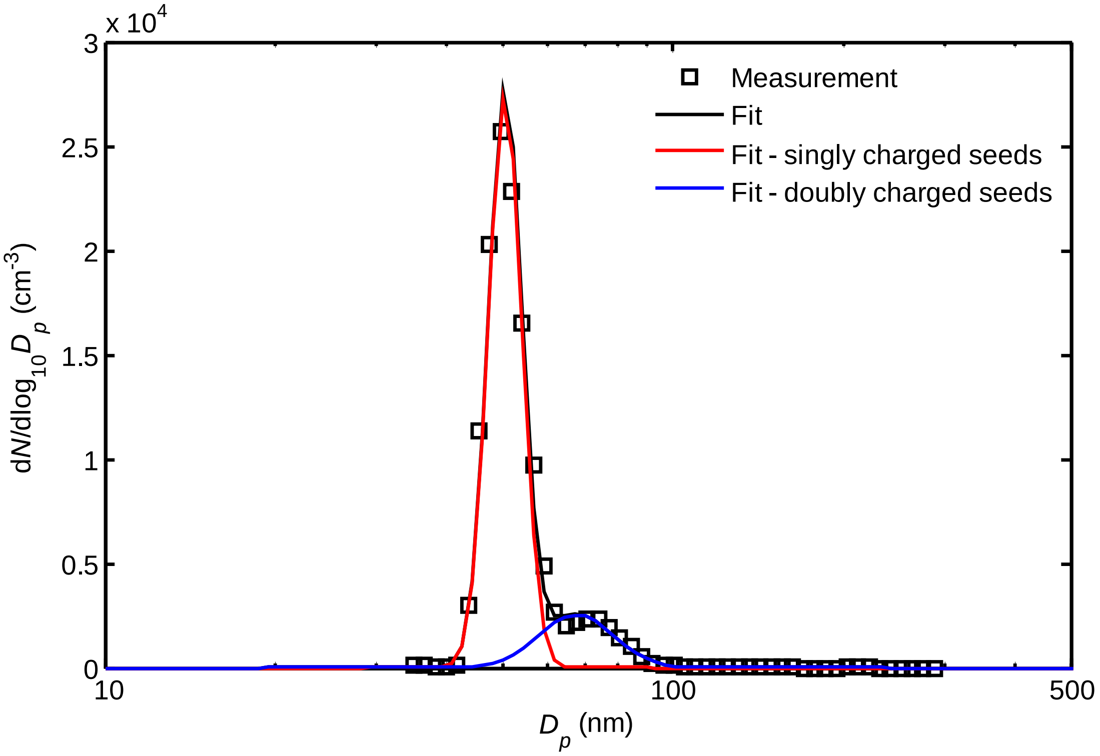

Figure S2. An example of measured size distribution of ammonium sulfate seeds. Also shown are the lognormal fits of all, singly-charged, and doubly charged seeds.

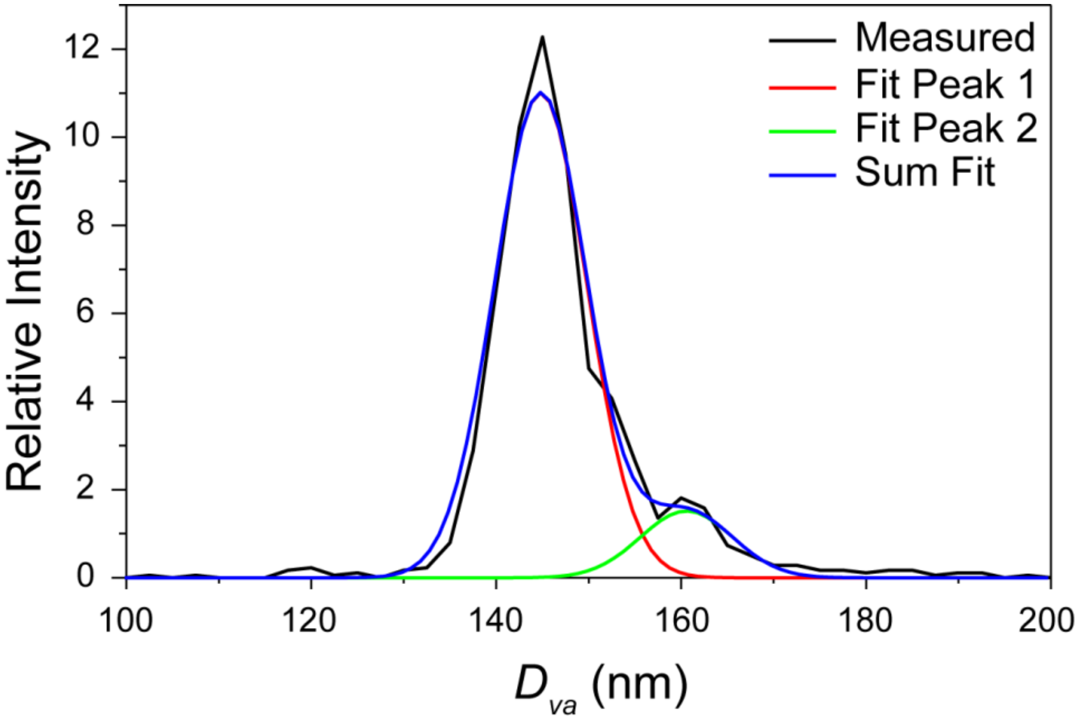

Figure S3. An example D_{va} distributions of 100 nm SOA-coated AS particles classified by a DMA during the experiment on June 21, 2015. Also shown are fitted peaks corresponding to particles grown on singly and doubly charged AS seeds, respectively.

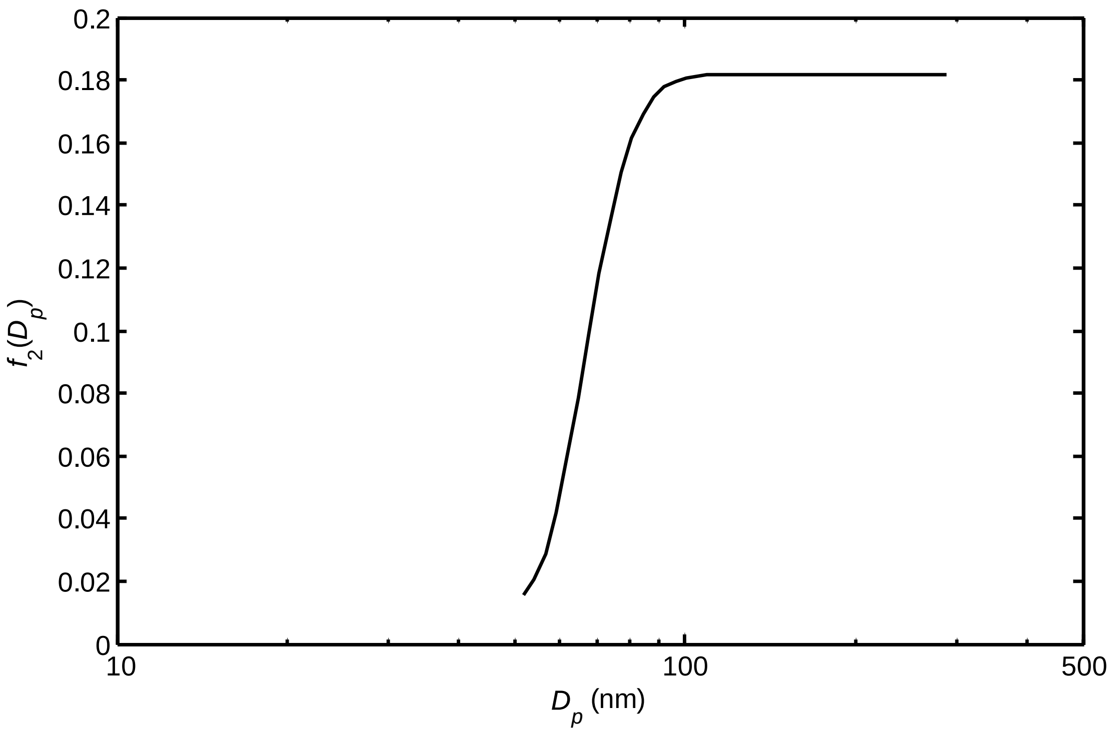

Figure S4. The value of $f_2(D_p)$ as a function of D_p derived from seed particle size distributions using τ of 4.3 hours, and a set of representative parameters (i.e., α = 0.027 h^{-1}, β_A=1.5 e-6 $\mu m^2 s^{-1}$, β_B=2.5 e-7 $\mu m^2 s^{-1}$, λ_A = 17 nm, and λ_A = 21 nm) reported in Seinfeld et al. (2003)

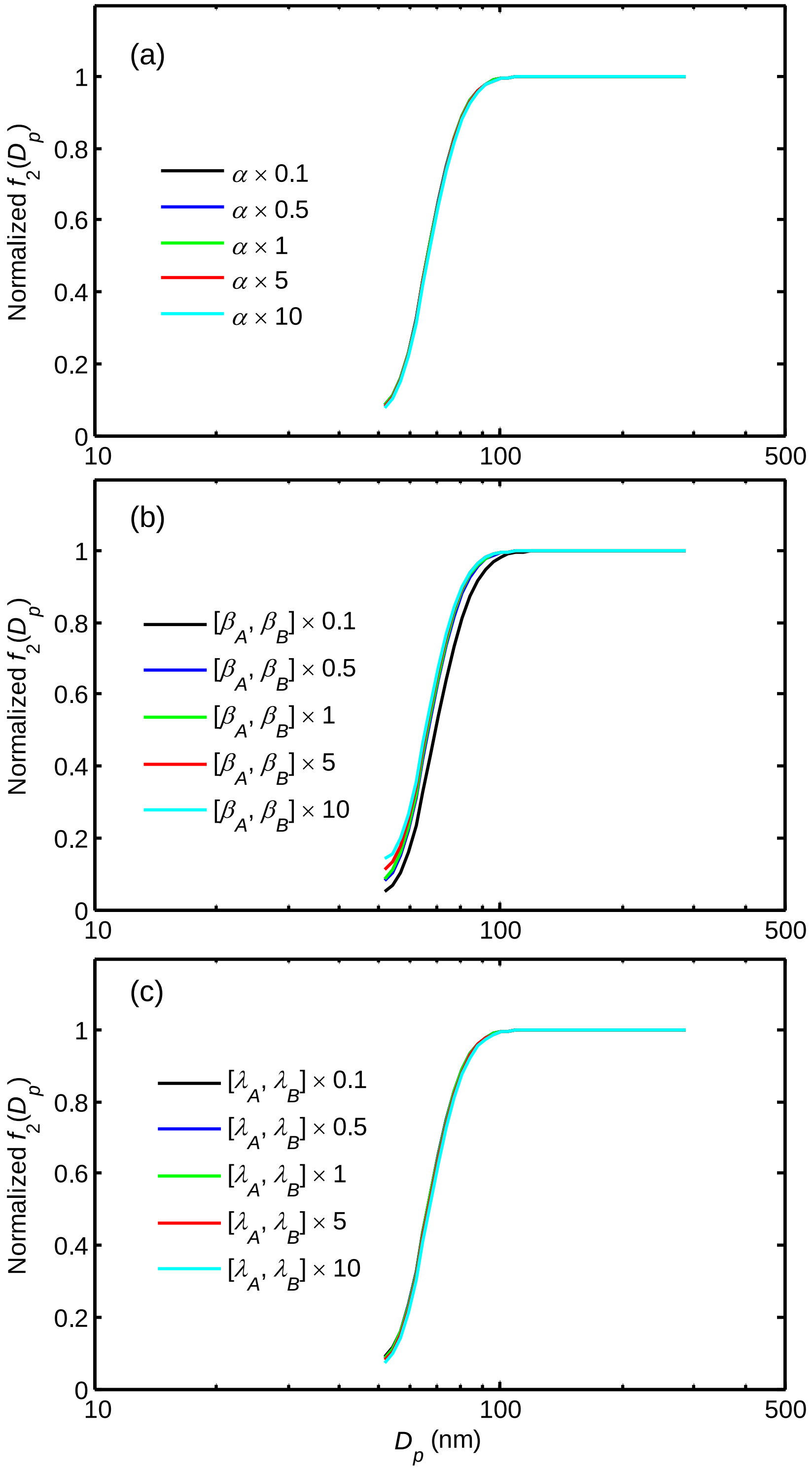

Figure S5: The dependences of $\overline{f_2(D_p)}$ on values of (a) α, (b) β_i, and (c) λ_i , respectively.

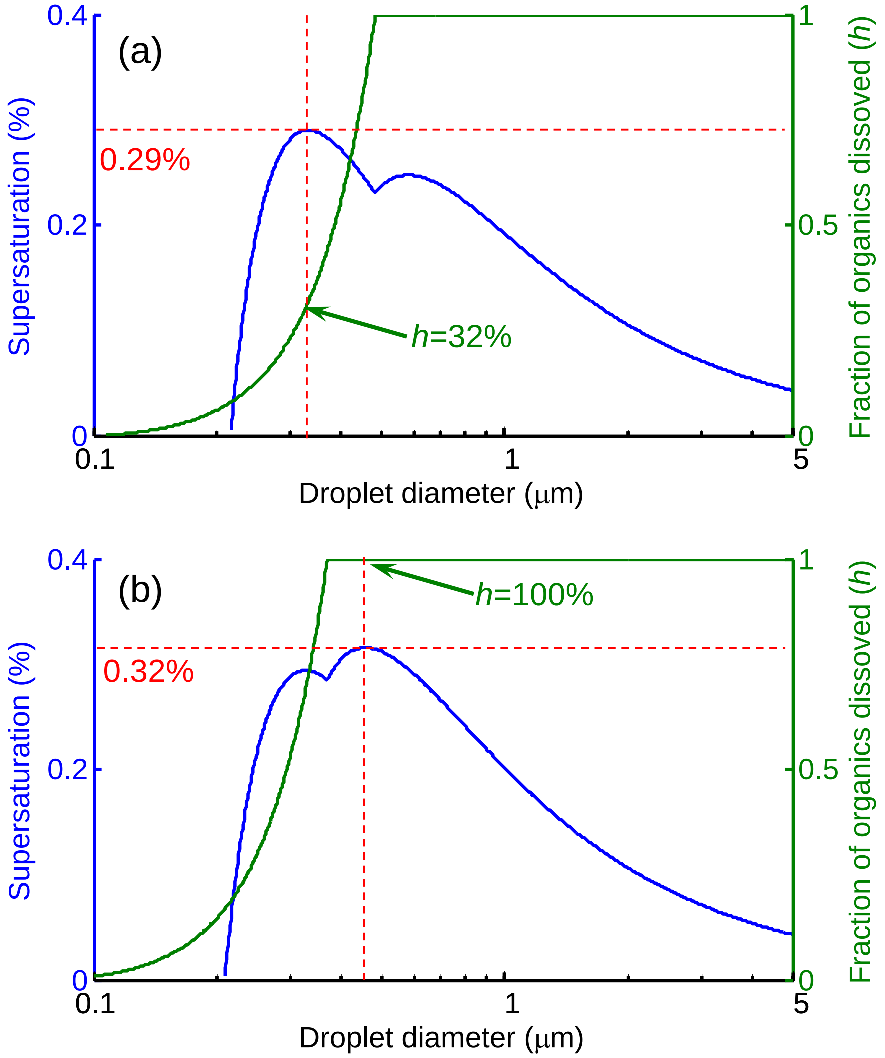

Figure S6: Example of calculated Köhler curve (blue line) for particles consisting of sulfate and sparing soluble organics with solubility of 0.01. The volume of sulfate inside the particles is equivalent to a 50 nm sulfate particle and the sulfate volume fractions are 0.1 (a) and 0.2 (b) respectively. Also shown is the fraction of organics dissolved (*h*) as a function of droplet diameter, the critical supersaturation (i.e., peak of the Köhler curve) and the corresponding *h*.

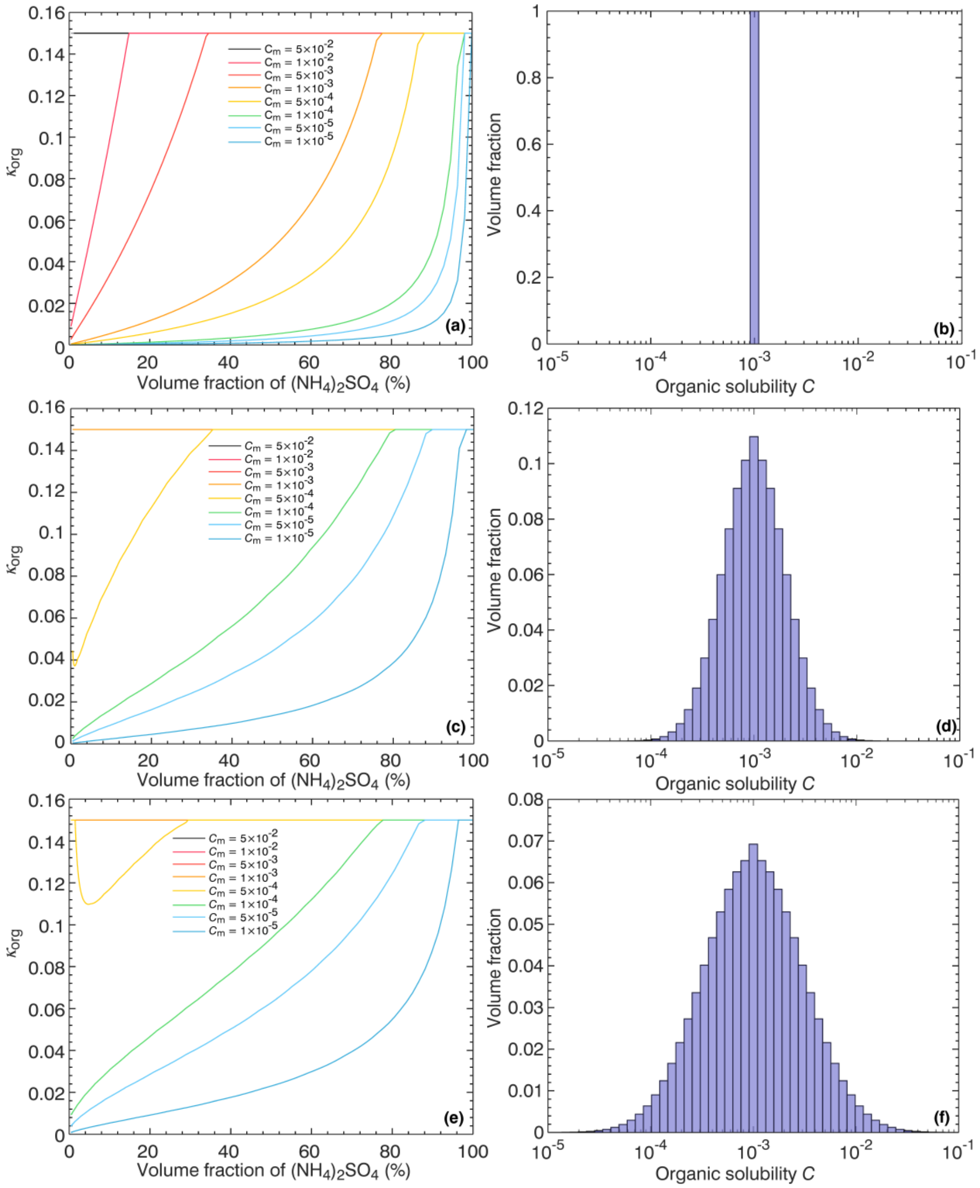

Figure S7. Panels (a), (c), and (e): Simulated effective organic hygroscopicity for particles grown from 50 nm ammonium sulfate seeds by condensation of secondary organic species with $\kappa_{org,intr}$ = 0.15. The effective organic hygroscopicity is shown as a function of sulfate volume fraction for organic solubility distributions C with mode solubility (C_m) ranging from 5×10^{-2} to 1×10^{-5}. Panels (b), (d), and (f): examples of solubility distribution centered at $C_m = 1\times10^{-3}$ for the 61 component mixture. The 61 components are assumed to behave independently of one another as in a mixture of non-interacting solids (i.e., solubility not affected by the presence of other component, and the dissolution behavior of each component is the same as their behavior as pure components).

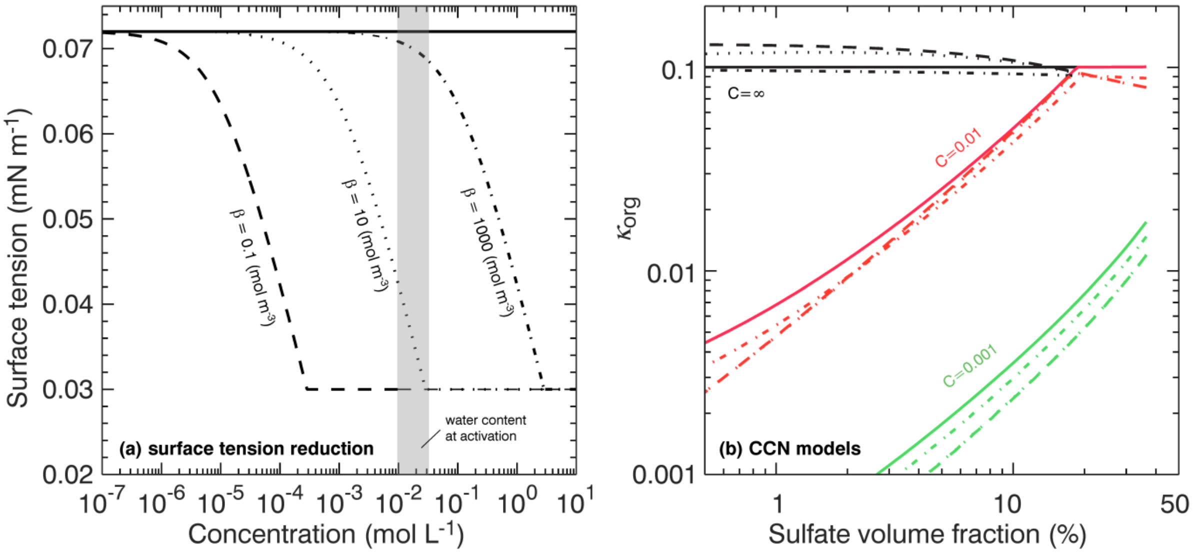

Figure S8. Model calculations combining limited solubility and surface tension reduction. (a) Hypothetical Szyskowski surface tension isotherms assuming $\alpha = 1.8 \times 10^{-4}\, m^3\, mol^{-1}$, $\Gamma_{max} = 5 \times 10^{-6}\, mol\, m^{-2}$, $\beta = \{0.1, 10, 1000\}\, mol\, m^{-3}$, and $cmc = 0.03\, J\, m^{-2}$. (b) Modeled κ_{org} assuming $C = \{\infty, 0.01,\ 0.001\}$ (colors). Solid line corresponds to constant surface tension $\sigma = 0.072\, J\, m^{-2}$. Dashed and dotted lines assume surface tension reduction as shown in (a).

References in Supplementary Information:

Allan, J. D., Delia, A. E., Coe, H., Bower, K. N., Alfarra, M. R., Jimenez, J. L., Middlebrook, A. M., Drewnick, F., Onasch, T. B., Canagaratna, M. R., Jayne, J. T., and Worsnop, D. R.: A generalised method for the extraction of chemically resolved mass spectra from aerodyne aerosol mass spectrometer data, J. Aerosol Sci., 35, 909-922, 2004.

Asa-Awuku, A., Engelhart, G. J., Lee, B. H., Pandis, S. N., and Nenes, A.: Relating CCN activity, volatility, and droplet growth kinetics of beta-caryophyllene secondary organic aerosol, Atmos. Chem. Phys., 9, 795-812, 2009.

Bertram, A. K., Martin, S. T., Hanna, S. J., Smith, M. L., Bodsworth, A., Chen, Q., Kuwata, M., Liu, A., You, Y., and Zorn, S. R.: Predicting the relative humidities of liquid-liquid phase separation, efflorescence, and deliquescence of mixed particles of ammonium sulfate, organic material, and water using the organic-to-sulfate mass ratio of the particle and the oxygen-to-carbon elemental ratio of the organic component, Atmos. Chem. Phys., 11, 10995-11006, 2011.

Bilde, M. and Svenningsson, B.: CCN activation of slightly soluble organics: the importance of small amounts of inorganic salt and particle phase, Tellus B, 56, 128-134, 2004.

Canagaratna, M. R., Jimenez, J. L., Kroll, J. H., Chen, Q., Kessler, S. H., Massoli, P., Hildebrandt Ruiz, L., Fortner, E., Williams, L. R., Wilson, K. R., Surratt, J. D., Donahue, N. M., Jayne, J. T., and Worsnop, D. R.: Elemental ratio measurements of organic compounds using aerosol mass spectrometry: characterization, improved calibration, and implications, Atmos. Chem. Phys., 15, 253-272, 2015.

Chen, Q., Liu, Y. J., Donahue, N. M., Shilling, J. E., and Martin, S. T.: Particle-Phase Chemistry of Secondary Organic Material: Modeled Compared to Measured O:C and H:C Elemental Ratios Provide Constraints, Environ. Sci. Technol., 45, 4763-4770, 2011.

Collins, D. R., Flagan, R. C., and Seinfeld, J. H.: Improved inversion of scanning DMA data, Aerosol Sci. Technol., 36, 1-9, 2002.

DeCarlo, P. F., Kimmel, J. R., Trimborn, A., Northway, M. J., Jayne, J. T., Aiken, A. C., Gonin, M., Fuhrer, K., Horvath, T., Docherty, K., Worsnop, D. R., and Jimenez, J. L.: Field-Deployable, High-Resolution, Time-of-Flight Aerosol Mass Spectrometer, Anal. Chem., 78, 8281-8289, 2006.

Forestieri, S. D., Staudt, S. M., Kuborn, T. M., Faber, K., Ruehl, C. R., Bertram, T. H., and Cappa, C. D.: Establishing the Impact of Model Surfactants on Cloud Condensation Nuclei Activity of Sea Spray Aerosols, Atmos. Chem. Phys. Discuss., 2018. https://doi.org/10.5194/acp-2018-5207, 2018.

Holmes, J. R., Obrien, R. J., Crabtree, J. H., Hecht, T. A., and Seinfeld, J. H.: MEASUREMENT OF ULTRAVIOLET-RADIATION INTENSITY IN PHOTOCHEMICAL SMOG STUDIES, Environ. Sci. Technol., 7, 519-523, 1973.

Hori, M., Ohta, S., Murao, N., and Yamagata, S.: Activation capability of water soluble organic substances as CCN, J. Aerosol Sci., 34, 419-448, 2003.

Kuwata, M., Zorn, S. R., and Martin, S. T.: Using Elemental Ratios to Predict the Density of Organic Material Composed of Carbon, Hydrogen, and Oxygen, Environ. Sci. Technol., 46, 787-794, 2012.

Lindinger, W., Hansel, A., and Jordan, A.: On-line monitoring of volatile organic compounds at pptv levels by means of proton-transfer-reaction mass spectrometry (PTR-MS) - Medical applications, food control and environmental research, International Journal of Mass Spectrometry, 173, 191-241, 1998.

Mei, F., Setyan, A., Zhang, Q., and Wang, J.: CCN activity of organic aerosols observed downwind of urban emissions during CARES, Atmos. Chem. Phys., 13, 12155-12169, 2013.

Noziere, B., Baduel, C., and Jaffrezo, J. L.: The dynamic surface tension of atmospheric aerosol surfactants reveals new aspects of cloud activation, Nature Communications, 5, 2014.

Ovadnevaite, J., Zuend, A., Laaksonen, A., Sanchez, K. J., Roberts, G., Ceburnis, D., Decesari, S., Rinaldi, M., Hodas, N., Facchini, M. C., Seinfeld, J. H., and Dowd, C. O.: Surface tension prevails over solute effect in organic-influenced cloud droplet activation, Nature, 546, 637-641, 2017.

Petters, M. D. and Kreidenweis, S. M.: A single parameter representation of hygroscopic growth and cloud condensation nucleus activity - Part 2: Including solubility, Atmos. Chem. Phys., 8, 6273-6279, 2008.

Petters, M. D. and Kreidenweis, S. M.: A single parameter representation of hygroscopic growth and cloud condensation nucleus activity - Part 3: Including surfactant partitioning, Atmos. Chem. Phys., 13, 1081-1091, 2013.

Petters, M. D., Kreidenweis, S. M., Snider, J. R., Koehler, K. A., Wang, Q., Prenni, A. J., and Demott, P. J.: Cloud droplet activation of polymerized organic aerosol, Tellus B, 58, 196-205, 2006.

Petters, M. D., Kreidenweis, S. M., and Ziemann, P. J.: Prediction of cloud condensation nuclei activity for organic compounds using functional group contribution methods, Geosci. Model Dev., 9, 111-124, 2016.

Petters, S. S. and Petters, M. D.: Surfactant effect on cloud condensation nuclei for two-component internally mixed aerosols, J. Geophys. Res., 121, 1878-1895, 2016.

Prisle, N. L., Raatikainen, T., Laaksonen, A., and Bilde, M.: Surfactants in cloud droplet activation: mixed organic-inorganic particles, Atmos. Chem. Phys., 10, 5663-5683, 2010.

Raatikainen, T. and Laaksonen, A.: A simplified treatment of surfactant effects on cloud drop activation, Geosci. Model Dev., 4, 107-116, 2011.

Rothfuss, N. E. and Petters, M. D.: Influence of Functional Groups on the Viscosity of Organic Aerosol, Environ. Sci. Technol., 51, 271-279, 2017.

Ruehl, C. R., Davies, J. F., and Wilson, K. R.: An interfacial mechanism for cloud droplet formation on organic aerosols, Science, 351, 1447-1450, 2016.

Seinfeld, J. H., Kleindienst, T. E., Edney, E. O., and Cohen, J. B.: Aerosol growth in a steady-state, continuous flow chamber: Application to studies of secondary aerosol formation, Aerosol Sci. Technol., 37, 728-734, 2003.

Shulman, M. L., Jacobson, M. C., Carlson, R. J., Synovec, R. E., and Young, T. E.: Dissolution behavior and surface tension effects of organic compounds in nucleating cloud droplets, Geophys. Res. Lett., 23, 277-280, 1996.

Topping, D., Connolly, P., and McFiggans, G.: Cloud droplet number enhanced by co-condensation of organic vapours, Nature Geoscience, 6, 443-446, 2013.

Zelenyuk, A., Imre, D., Wilson, J., Zhang, Z., Wang, J., and Mueller, K.: Airborne Single Particle Mass Spectrometers (SPLAT II & miniSPLAT) and New Software for Data Visualization and Analysis in a Geo-Spatial Context, Journal of The American Society for Mass Spectrometry, 26, 257-270, 2015.

Zelenyuk, A., Yang, J., Song, C., Zaveri, R. A., and Imre, D.: A New Real-Time Method for Determining Particles' Sphericity and Density: Application to Secondary Organic Aerosol Formed by Ozonolysis of α-Pinene, Environmental Science & Technology, 42, 8033-8038, 2008a.

Zelenyuk, A., Yang, J., Song, C., Zaveri, R. A., and Imre, D.: A New Real-Time Method for Determining Particles' Sphericity and Density: Application to Secondary Organic Aerosol Formed by Ozonolysis of alpha-Pinene, Environ. Sci. Technol., 42, 8033-8038, 2008b.